ELASTIC ANALYSIS OF THE LOOP TACK TEST FOR PRESSURE SENSITIVE ADHESIVES

NuRocha Lyn Williams

Thesis submitted to the Faculty of the
Virginia Polytechnic Institute and State University
In partial fulfillment of the requirements for the degree of

MASTER OF SCIENCE
IN
CIVIL AND ENVIRONMENTAL ENGINEERING

Approved by:

_____
Raymond H. Plaut, Chairman

_____ _____
Siegfried M. Holzer David A. Dillard

June 29, 2000
Blacksburg, Virginia

Key Words: Adhesion, Elastica, Loop Tack Test, Pressure Sensitive Adhesives

ELASTIC ANALYSIS OF THE LOOP TACK TEST FOR PRESSURE SENSITIVE ADHESIVES

NuRocha Lyn Williams

Raymond H. Plaut, Chairman
Civil and Environmental Engineering

(ABSTRACT)

The loop tack test measures the tack (instant grip) of an adhesive. An analytical model of this test seems to be lacking and is the subject of this research. The strip is investigated using several mathematical formulations, and the solutions are obtained numerically. The loop is created from a flexible elastic strip that is bent into a teardrop shape, with its ends clamped together. The strip is tested in a cycle, in which the loop is first pushed onto the surface, compressing the adhesive. Then the loop is pulled up, and gradually debonds from the substrate. The loop is assumed to be nonlinearly elastic and inextensible.

The mechanics of the loop tack test are studied in order to determine the impact of various factors on adhesive performance. These factors include the stiffness of the backing, the stiffness and thickness of the adhesive, the elongation of the adhesive before debonding, and the contact time.

The relationship between the applied force and the vertical deflection of the loop's ends is determined, as well as that between the applied force and the contact length. Also, the maximum "pull – off" force needed to remove the substrate from the loop is obtained from the results. Shapes of the loop during the cycle are found.

This research will increase understanding of the behavior of the adhesive and backing during the loop tack test. With the computer model that has been developed, any set of parameters and conditions can be analyzed, and improvements can be made in the test procedure.

Acknowledgements

I praise and thank him for allowing me to write and finish this thesis

Many thanks to Dr. Plaut for all of his help, guidance and patience with me during my research and thesis writing. I would also like to thank Dr. David Dillard and Dr. Siegfried Holzer for their encouragement, and for serving as my committee members.

Special thanks to the National Science Foundation (Grant CMS-9713949), and the Adhesion and Sealant Council Education Foundation for providing funding to complete this research.

Thank you to my family, Dad, Mom, Dana and Galen for their continuing support, encouragement, and phone calls. Thanks to Uncle Earnest for the phone calls and emails. Thanks to the Crawford family for providing potato chips. Thanks to Aunt Dolores for her mentoring advice. Thanks to Uncle Charlie and Aunt Bessie, for making the special effort to come and visit me here for graduation, even though I wasn't quite done.

Thanks to the girls for the Monday night dinners, which provided nourishment so I could have strength to write late at night. Thanks to Amy Dalrymple for introducing and explaining Mathematica to me. Thanks to LIGHT for putting up with my craziness at devotionals. Thanks to April Henderson, Dave Henderson and Brownie for making Wednesdays family day. Thanks to James Bryant for helping with Word. Thanks to John Ryan, Rich Meyerson, Anthony Farmer, Tony Temeles, Mike Neubert, and Amy Dalrymple, for the backpack, it has carried many things. Thanks to Barrett and Karen Coffman for the calculator, without which this engineer is in trouble. Thanks to all those who asked questions and made me actually explain what this thesis is all about.

Table of Contents

Table of Contents, Continued

List of Figures

Figures, Continued

Figures, Continued

Figures, Continued

List of Tables

Chapter 1

Introduction and Literature Review

1.0 Introduction

Adhesives are everywhere. The vast applications of adhesives in our everyday lives are not even recognized. Where did these adhesives come from and how have they come to play such an important role in our lives? The first adhesives came from the surrounding environment. Spider webs, plant and asphaltic materials that trap insects, birds and small mammals are several examples of sticky things in nature (Keimel, 1994). From man's earliest times, some sort of adhesive was used. In Biblical times, when Noah built the ark, he used an adhesive or sealant to seal and waterproof the ship. Also, in the construction of the Tower of Babel it is thought that bitumen was used as mortar. As history continues, there are even more examples of the beginning of adhesive technology. The historic Egyptians used crude animal and casein glue to laminate wood for bows and furniture, while the Greeks and Romans mixed lime with volcanic ash and sand to create a material still known as pozolanic cement (Keimel, 1994). From these humble beginnings, of using natural resources, the adhesive technology that we have today was born.

1.1 Pressure Sensitive Adhesives

This thesis focuses on one particular type of adhesive: pressure sensitive adhesives (PSA's). Pressure sensitive adhesives, also known as permanent-tack adhesives, are defined as adhesives that are able to develop measurable adhesion to a surface simply upon contact or by the application of a light pressure. Generally, no chemical reaction takes place between the adhesive and adherend, no curing of the adhesive is necessary, and no solvent is lost during the adhesion process (Creton and Leibler, 1996). The Pressure Sensitive Tape Council (PSTC) determined that pressure sensitive adhesives should characteristically display the following properties (Pocius, 1997):

1. Aggressive and permanent tack
2. Adheres with no more than finger pressure

3. Requires no activation by any energy source
4. Has sufficient ability to hold onto the adherend
5. Has enough cohesive strength to be able to be removed cleanly from the adherend.

There are several general categories of PSA's, which include:

1. Removable adhesives –These are PSA's for which a high compliance is required in order to establish contact very easily, but conversely low adhesion is necessary. In addition, the separation must be completely adhesive to avoid residue of the adhesive layer on the substrate. The most widely known example is the Post-It® note[1].
2. General-purpose, semi-permanent adhesives – This is the most common type of adhesive. Medium compliance and relatively good adhesion are characteristic. There is no long-term resistance to the environment because the lifetime use is typically a few months. The adhesive is considered to be permanent if, upon removal the backing fails before the adhesive bond. Examples of this type include standard office tape and labels.
3. Permanent, semi-structural adhesives – These adhesives exhibit very high adhesion and creep resistance, as well as good resistance to the environment. For this application, the PSA's ease of application is the motivation to use it as a substitute for more conventional adhesives (Creton and Leibler, 1996).

The advantages of using pressure sensitive adhesives include that there is no storage problem, no mixing or activation is necessary in bond formation, no waiting is involved in this bond formation, and often the bond created by the PSA is readily reversible. Disadvantages of using pressure sensitive adhesives include that the adhesive strength, especially for peeling and shearing, is low, bonds cannot be easily formed on unsuitable or rough surfaces, and pressure sensitive adhesives are expensive in terms of cost per unit bond area (Aubrey, 1992).

[1] Post-It note is a registered trademark of the 3M Corporation

1.1.1 History

The first use of natural rubber-based "tacky" adhesives on a backing is credited to Henry Day, who was issued United States patent number 3,965 in 1845. James Corbin of the Minnesota Mining and Manufacturing Co. (now 3M), in a 1952 paper entitled, "Practical Applications of Pressure-Sensitive Adhesives," wrote that 1925 is considered to be the birthdate of the pressure-sensitive industry. Prior to that time, both cloth-backed surgical tapes and cloth-backed friction tapes for use by electricians were in limited use (Keimel, 1994).

The first formulations of pressure sensitive adhesives used natural rubber-based adhesive. Natural rubber chemically is poly(cisisoprene) and is obtained from the Hevea rubber plant as a natural latex. This rubber served as the basis for most, if not all, of the early PSA products and dominated the market until after World War II (Goulding, 1994). Chemical solutions for PSA labels and tapes are primarily blends of rubber and tackifying materials such as resins. The low molecular weight polysobutylenes find use as permanent tackifiers and modifiers, while the higher molecular weight products serve as rubbery base materials. Tackifiers and modifiers often enhance tack and softness; they can also contribute to adhesion by improving wetting of the substrate (Hammond, 1982). Natural rubber-based PSA's are still used in pressure sensitive adhesive tape (PSAT) applications, including masking tape, and exhibit excellent removability after painting and baking. Tapes and adhesives containing natural rubber were widely used because this material is relatively inexpensive and can achieve a high peel strength. One flaw of the product is that the adhesive has a tendency to yellow and to crosslink, becoming brittle, making it unstable to long-term exposure to the environment (Pocius, 1997). After World War II, the adhesive formulation changed. As the price of solvents increased and as the environmental opposition to the use of solvents mounted, adhesives without natural rubber and solvents were put on the market. There were a large number of elastomers, such as synthetic rubber and other polymers now available, which made way for water-based and hot-melt type adhesives.

The largest application areas for pressure sensitive adhesives include packaging tapes and insulation, followed by self-adhesive labels. Other applications of these adhesives

include: self-adhesive floor tiles, adhesives for décor papers and flypapers, gloss lamination (application of thin films of polyester or polyolefin over printed paper to enhance gloss and protect print), and disposable diapers (Pizzi and Mittal, 1994; Goulding, 1994).

1.1.2 Testing Procedures

Testing products creates a standard by which to determine if one product is better than another in accomplishing the task that it was created for. One adhesive consultant, Chemsultants, had an article on their web page about benchmark testing. This article defined benchmark testing as a reference point for comparing current products and judging future products or services. The article went on to say that testing should serve as a tool that provides insight into the strengths and weaknesses of current technology and should be used as a baseline for future decisions and growth. Continuing, the article named four qualities of good benchmark testing. In summary, these qualities include that testing must be objective and quantifiable in a reproducible manner. Also, the properties being tested must be significant, in other words there should be a reason for conducting the test. Furthermore, the product tested must be representative of its group, a properly documented random sample (Eppink and Frye, 1999).

PSA testing must be performed under controlled conditions in order to produce accurate results. The geometry of the PSA must be maintained throughout the test, in order to generate reliable results. It is also critical that the proper equipment and environmental conditions are used for each test to assure that variables that negatively impact data are minimized (Eppink and Frye, 1999).

Tack, peel, and shear strength are the main characteristics that PSA's are tested for. Testing these characteristics provides an understanding of how quickly and how firmly the adhesive will stick and how strongly it will resist any applied shear forces. There are tests to measure each of these quantities. Peel strength is the resistance of a tape joint to peeling under specified conditions (Aubrey, 1992). Usually this property is tested using either the 90 or 180 degree peel test. In the 180° peel test, the PSA tape is applied to the stiff adherend, the tape is then folded back over itself, forming a long tab. The top of the stiff adherend is clamped into a tensile testing machine, and so is the end of the long tab.

After achieving this initial configuration, the adhesive tape is then pulled off at 180°. Though the test is named the 180° test, the actual angle of peel depends on the backing stiffness and thickness. The 90° peel test is conducted in a similar fashion to the 180° test, except that an angle of 90° is maintained throughout the test.

Shear strength is the ability of the adhesive to withstand creep, which is regarded as the increase in strain with time after stress is suddenly applied and maintained constant (Hammond, 1982). This quality is usually tested using a set-up where a standard area of the coated film is bonded to a steel plate or standard cardboard. A fixed load is applied and the time till failure is recorded. This test can be conducted at various temperatures, depending on the properties needed in the final application (Pizzi and Mittal, 1994). This test gives little information about the intrinsic properties of the adhesive because there are at least three possible modes of failure. The adhesive may undergo a true shear failure. However, the tape may also lift intact from the plate or peeling may occur from the unloaded end of the tape, due to low adhesion accompanied by a turning moment induced from elastic deformation of the backing (Aubrey, 1992).

The measurements of peel and shear depend greatly on the amount that the adhesive wets the surface. Because of this, one author suggests that the roll-down methodology be used. This requires the tape to be laid down on the substrate with little or no applied pressure. A roller of known weight and dimensions is rolled over the tape at a specified rate and a pre-determined number of times up and down the tape. Roll down controls the degree the PSA wets the substrate, and should give more accurate measurements of the specific quantity being measured (Pocius, 1997).

1.2 What is Tack?

In the various applications for PSA's the adhesive must make intimate contact with the adherend and must be capable of wetting it out in order to be effective in "sticking" (Johnston, 1983a). For this reason, the measurement of tack and the factors affecting its behavior have been studied and analyzed. Tack is defined as wet grab, quick stick, that which allows a pressure sensitive adhesive to adhere to a surface under very slight pressure (Pressure Sensitive Tape Council), initial adhesion, finger tack, thumb tack, quick grab, quick adhesion, and wettability (Johnston, 1983a). The American Society for

Testing and Materials (ASTM) defines tack as the force required to separate an adherend and adhesive at the interface shortly after they have been brought rapidly into contact under light load of short duration (Johnston, 1983a). Another definition of tack defines tack as the property whereby an adhesive will adhere tenaciously to any surface it comes in contact with, under light pressure. The strength of the bond will be greater under increasing pressure (Hammond, 1982). Tackiness can be classified into two groups: the wetting against the solid body to be taped, and the resistance against the detachment of the tape from the taped solid body (Kamagata et al., 1970). In addition to having so many definitions of tack, there are also several different forms of tack. These forms are as defined in the following:

Cohesive Tack – involves the bulk flow of one or both materials during separation, and applies to materials like printing inks, paints, syrups, and is dependent on the internal strength of the adhesive (Hammond, 1982). Any resistance to separation is governed by viscous flow according to the Stefan equation (Aubrey, 1992).

Adhesive Tack – involves a separation at the original interface between the materials. This kind of tack applies particularly to pressure sensitive adhesives, although such adhesives may display cohesive tack under extreme conditions of rate or temperature (Aubrey, 1992).

Autohesive Tack – involves two elastomeric materials of essentially the same composition and is considered to be the specific adhesion of the adhesive to itself, which is often referred to as the true tack or building tack (Hammond, 1982). In this case separation may be either adhesive (usually after short times of contact) or cohesive (usually after long times of contact). Autohesive tack is important in the use of contact adhesives and in plying together rubber surfaces, for example in the manufacture of tires (Aubrey, 1992).

1.2.1 Factors Influencing Tack

Anyone can tell someone else whether or not a material in question is “sticky,” but actually testing is not that simple and requires accurate measurements. Tack measurements are necessary because they indicate the bonding and unbonding processes

that an adhesive experiences, and how successful the material tested should be in practical applications. One reason tack must be measured is because the control of tack is essential in many bonding processes. Too great a tack may cause nearly as many problems as too low of a tack (Duncan et al., 1999). Though tack is a necessary quantity to know in order to determine whether or not an adhesive is acceptable for certain applications, it is often difficult to quantify because there are many factors that influence its measurement.

Some of the factors that influence tack are the adhesive used, contact load, dwell time, adherend temperature, humidity, and the adhesive's flow characteristics (Hu et al., 1998). Creton and Leibler (1996) attempted to better understand the dependence of tack on the pressure and contact time, and to relate quantitatively the results to the molecular structure of the adhesive and the roughness of the substrate. In drawing conclusions from their research, the data suggests that tack is dependent on these variables, and that the tack force is directly proportional to the true area of contact. These findings are substantiated by other findings in the literature. Gay and co-authors determined that surface roughness and true area of contact are crucial to determine the quality of contact and thereby the intensity of adhesion (Gay et al., 1999).

Continuing, the factor that seems to affect tack the most is the adhesive and backing, together as a system. Most adhesion properties are influenced by the nature and thickness of the adhesive and backing film layers and by the stiffness or flexibility of the tape backing. This makes the results obtained not only intrinsic properties of the adhesive, but they become properties of the composite tape system (Aubrey, 1992; Satas, 1989).

Tack is considered a viscoelastic property because sometimes the adhesive being tested may tend to act like a liquid even though it is a solid, creating a time dependence. A viscoelastic liquid is one that after deformation partially returns to its original shape when an applied stress is released (Fox and McDonald, 1992). The tack of natural rubber is determined by the response of a viscoelastic material to deformation under the effect of pressure, and the adhesive thickness is an important parameter. The minimum coating weight of an adhesive is determined by that thickness which will allow sufficient

viscoelastic response to form adequate tack properties; thickness is also important for elastic behavior (Hammond, 1982). Tack is essentially a measure of viscous flow under conditions of fast strain rates and low stress magnitudes, while shear adhesion measures viscous flow at low strain rates and intermediate stress magnitudes (Hammond, 1982). This current research ignores viscoelastic effects, but they are important to predict the dependence of the tack energy on contact time and debonding speed.

Tack is also a process in which, for a high tack value and high peel strength, a polymer must dissipate a large amount of deformation energy during debonding. Researchers suggest that this energy dissipation is connected with the formation and growth of fibrils during bond separation. Fibrillation seems to be crucial to the peel strength and the tack of polymers to be used as pressure sensitive adhesives. A three-step process, fibrillation, includes the formation of fibrils, their deformation, and their debonding. As a viscoelastic phenomenon fibrillation strongly depends on temperature and the rate of separation (Zosel, 1998). This characteristic is not directly covered by this current research, but its effects have been seen.

1.2.2 History of Measuring Tack

One of the first tests developed to measure tack was the Thumb Tack Test. During this test the operator presses his or her thumb against the adhesive surface and then removes it. The sensation to the operator is used to judge the tack of the adhesive. After time, the operator develops an "educated" thumb and is able to differentiate between various grades of adhesives with accuracy. However, this test is not effective because the results depend on the experience level of the operator doing the testing. Though the test distinguishes that one adhesive is "stickier" than another, the contact area is uncontrolled and the test may not indicate how the tape will perform in practical use (Johnston, 1983a).

The Matibes Ball Tack Test evolved out of the concept behind the Thumb Tack Testers. Here a steel ball is suspended in an annulus from a strain gauge. The adhesive being tested is brought into contact for 2 to 3 seconds, which raises the ball from the annulus, so that the applied pressure is the weight of the ball. Next, the adhesive is moved away from the ball at a rate of 12 in./min until the ball returns to the annulus. The force

required to separate is taken as the tack value. The disadvantage of this method is that the contact area varies, depending on the ease of adhesive deformation (Johnston, 1983).

There are various forms and methods for the loop tack test as it has developed over the years. One of the predecessors of the modern-day loop tack test came around 1950, with the use of the Loop or Strip Testing Method. In this test the set-up included a hinged metal box with a smooth lid. The lid was contacted with 1 square inch of the tape. After about 5 seconds the box lifted. Weights were added and the process repeated until the tape could not lift the box. The total weight recorded would be a measure of the tack. This method was not readily accepted because it is long and tedious, and the results are questionable (Johnston, 1983a).

Another predecessor of the loop tack test is the Self-Pressure Tack Tester developed by Nichiban. In this test 1 in. x 12 in. samples of tape are layered into a circular loop, hung on a peg, and attached to a tensile tester's upper jaws. A horizontal test plate mounted in the lower jaws is raised until the loop and test plate touch, then immediately separated at 12 in./min. The force required to separate the loop from the test plate is recorded as a measurement of tack. Problems with this method include that the control of area and dwell time is poor, and the flexibility of the backing affects the results (Johnston, 1983a).

The next testing method is the Morgan Quick Stick Test. During this test, the ends of a 1in. x 5 in. strip of tape are brought together with the adhesive exposed using a ¾ in. x 2½ in. strip of tape to secure the ends together. This sealed end is mounted in the upper jaws of a tensile tester while the lower jaws hold a 1/16 in. thick horizontal stainless steel plate. The lower jaws are raised at 50 in./min until 1 $in.^2$ of the loop contacts the steel plate. The lower jaws are then immediately removed at 12 in./min, and the force required to separate the lower and upper jaws is considered to be the tack value. This testing method shares the same disadvantages as the Nichiban Method as mentioned above (Johnston, 1983a).

Another test is the Chang Test, which is a modified 90° Peel Test, also known as the Kreck Test, by Kendall Co. Here a 1 in. x 12 in. to 15 in. strip of tape is laid without pressure onto a standard stainless steel test panel. The panel is mounted into a test jig, which ensures that the tape remains at a constant 90° when stripped from the panel at

12 in./min. Because the tape must maintain an angle of 90°, the jig must move the test panel at the same rate as the tape is being stripped. The Chang Test differs from the 90° peel test because the tape is laid on the test panel without any applied pressure, then peeled immediately at 90° (Johnston, 1983a).

One of the problems with the Chang Test can be seen with a Bond Stress Analyzer device, which is used in conjunction with a standard adhesion tester. With this equipment, it is possible to see the spectrum of forces at work, ahead of and following the point of peel. The Bond Stress Analyzer shows an area of compression just behind the peel, which results in automatic pressure application of the tape to the test panel, no matter how small the initial application pressure. This compression is in the nature of peeling and is affected by the degree of flexibility of the backing, so what is happening is that the tape is effectively applying itself to the panel with pressure immediately following the peel zone. In effect it becomes a 90° adhesion test (Pizzi and Mittal, 1994), and the additional pressures applied to the adhesive may affect the accuracy of the results.

Other tests that were used to examine the tack of an adhesive include Frank Wetzel's modification of the Controlled Rate of Extension Tester, and the Polyken Probe Tack Tester. Wetzel proposed a probe tack testing device that could be fit to the standard Controlled Rate of Extension tester. In this proposal, Wetzel used a 1/16 in. diameter brass probe attached to a known weight of 10 grams, which was then mounted in a metal housing so that it could slide freely vertically. An adhesive sample was mounted on a horizontal plate in the lower jaws of the tensile tester, and the probe unit was mounted in the upper arm attachment. The sample was brought into contact with the probe so that the full weight of the sliding probe assembly rested on the adhesive surface. The sample was then held for a controlled period of time and then withdrawn at a controlled rate. Usually the best results were found with a dwell time of 1 sec and a rate of contact and removal of 20 in./min, approximately 1 cm/sec. For the results to be gathered accurately, it was essential that a high-speed recorder or oscilloscope be used to observe the behavior. For the first time with the implementation of this test, there was an apparatus that could be used as a research tool (Johnston, 1983b).

Though the Wetzel apparatus gave fairly reliable results, the test was abandoned and replaced by the Polyken Probe Tack Tester, developed by Hammond of Kendall. It is considered to be a redesign of the Wetzel method into a relatively simple, inexpensive portable unit. For this case the probe is attached to a force gauge, and the adhesive sample being tested is attached to an annular weight to control the applied pressure. The dwell time and the rate of the test correspond with Wetzel's method, but the test area is approximately ten times larger. A Kendall Tester was developed for research investigations, and several types of testers have been developed along this same theme (Johnston, 1983b).

1.2.3 The Main Tests

There have been and still are many tests that measure tack. From those, there are three tests that are the most popular, as shown through their wide use and acceptance in the industry. The modern-day probe tack test is conducted by bringing the probe into contact with the adhesive tape, which is attached over an annular weight (giving contact pressure), maintaining contact for a pre-determined dwell time and then pulling off at the set separation speed. For this test, the tack measurement is defined as the maximum force measured while separating the surfaces. Tack usually increases with contact pressure and dwell time, and the value is expected to improve as the adhesive spreads (Duncan et al., 1999). Mechanical probe tack tests are intended to be simulations of thumb or finger tack tests (Satas, 1989). For the probe tack test, it is difficult to accurately control the variables: probe material and finish, probe diameter and shape, load on probe, thickness of adhesive, dwell time, rate of debonding of probe from the adhesive, and test temperature (Aubrey, 1992). One of the benefits of the probe tack test is that the effect of the tape backing is eliminated because the tape is either rigidly affixed to a steel plate or mounted on an annular ring of known weight (Pocius, 1997).

Another test commonly used to measure tack is the Roller Ball Test. There are several variations of this test, but each test operates on the same basic principles, with results being influenced by the adhesive thickness, the bonding of the adhesive to the backing, and the backing stiffness. A section of adhesive is placed on a ramp inclined at a predetermined angle. A single steel ball, or a series of steel balls with increasing

diameters one at a time, is released down the ramp. Tack of the adhesive is indicate by the distance the balls travel on the adhesive layer before stopping. The shorter the distance the ball travels, the greater the tack; the longer the distance, the lower the tack. Besides determining the tack, this test serves as an indicator of the softness and mass of the adhesive. The test is quick and easy to perform, but is not intended as an investigative tool, since the results do not correlate well with application results, and the test is unreliable for water-based systems (Roberts, 1997; Pizzi and Mittal, 1994). The rolling ball tack test was developed when most pressure-sensitive adhesives were composed from natural rubber and tackifying resins. With such adhesives, there is an approximate relation between rolling ball and thumb tack. For adhesives containing synthetic elastomers or single component adhesives, however, the results of rolling ball and thumb tack tests are not comparable. Many functional adhesives synthesized from acrylates and other monomers do not stop the ball in the maximum prescribed length of tape and thus have no apparent rolling ball tack (Hammond, 1982).

The loop tack test is another test that measures the tack of an adhesive and is the focus of this research. The test is set up with a 1 in. wide strip of backing, coated with adhesive. The strip is folded into a loop configuration with the adhesive exposed. This loop is then placed in a machine, a tensile tester, where it is pushed downward at a constant speed, the industry standard being 300 mm/min. The loop contacts the substrate, and wets out to a length of about 1 in.. The loop is then pulled upward at the same speed as it went downward, until it debonds from the substrate. The maximum force required to debond the loop is recorded as the tack value. Of the organizations that govern testing, several use the loop tack test as their means of measuring tack. These include American Society for Testing and Materials (ASTM), Tag & Label Manufacturers Institute (TLMI), and FINAT. The FINAT procedure follows the same process as mentioned above, but the specific language of the testing procedure includes the provision that the substrate be glass, while the other testing procedures use highly polished (non-rough) metal surfaces, such as aluminum, as the standard substrate. Unlike other tests, the loop tack test allows the combined behavior of the adhesive and the backing to be measured, since the stiffness of the backing material significantly affects the results. Advantages of the loop tack test include that it can be used over a wide range of adhesive types and is best for

distinguishing modes of failure (Eppink and Frye, 1999). Some disadvantages of the loop tack test are that even in a single test, the loop tested is subject to variable peel angles and contact times. The results of the test also suffer from the large influence of the stiffness or flexibility of the tape backing on the magnitude of the force measured. A cause of this influence is the compression zone that presses the adhesive into contact with the adherend just ahead of the zone where the tape is being peeled off, and the magnitude of the compression force depends on the backing properties. Loop tack tests have the advantage of requiring only simple fixtures mounted on standard tensile testers. Though tedious, the loop tack test is quite easy to carry out, and is somewhat reproducible. Loop tack tests can very effectively assess the tack of adhesives on film or sheet (paper) backings for applications that are closely approximated by test conditions.

1.3 Summary

There are many ways and formulations used to measure and determine tack. Quantifying tack often frustrates the industry, because tack is defined and measured in many, usually incomparable ways for different industrial applications. Therefore, measured values are often not transferable between applications, leading to retesting of the same properties (Duncan et al., 1999). There is very little consistency throughout the industry regarding the best way to measure tack. This is best shown from the results of Roberts' round-robin lab experiment, that had thirteen laboratories all test the same adhesives using the loop tack test. From this experiment it was found that, in most test cases, different labs achieved the same classification of the tack of an adhesive, but the manners in which this value was achieved varied tremendously. Since there are few specific instructions in the testing procedures and there is often confusion on which method is more accurate, there has been some discussion of creating a more standard practice of measuring tack so that experiments can be reproduced from lab to lab with consistent results (Roberts, 1999).

Many of the topics discussed in this chapter came as the result of laboratory testing. There have been several attempts to look at the loop tack test from a more mathematical standpoint. Authors such as Duncan and Hu explored the use of finite element analysis to predict the stresses and deflections in the loop tack test. Crosby and Shull (1999) also tried to create a numerical method to compare with laboratory results. These models

seem to focus more on the stress and strain in the testing system. The research in this thesis focuses on the physical factors that affect the loop tack test. The model created seeks to predict the behavior of the loop throughout the test without having to run the actual test, by specifying the parameters of a particular tape to be tested.

Chapter 2

Objectives and Formulations

Though there are many descriptions of the loop tack test in the literature, there are few attempts at an analytical model of the system. This research seeks to create a method by which the loop tack test can be analyzed and various factors affecting the test's outcome can be examined, in order to increase understanding of the behavior of the adhesive and backing during the loop tack test.

2.1 System Assumptions

This research develops a computer model program by which a set of parameters and conditions can be analyzed, and seeks to obtain an accurate description of what will happen in actual lab tests. Several assumptions were made in generating the analysis program. The first is that the system is elastic. This assumption means that after going through the cycle of the test, the loop will return to its initial configuration. Another assumption that was made was that debonding occurs at a certain elongation of the adhesive. This elongation of the adhesive is dependent on the maximum pressure encountered at a location. It was also assumed that as the loop is bent, it maintains a continuous slope, and the strip is inextensible. Also, the weight of the loop is ignored, and the adhesive, when on the substrate, is modeled as an elastic foundation.

An elastica is defined by Antman and Pierce (1990) as "an unshearable incompressible column for which the bending couple depends linearly on the curvature." In the first part of this thesis, the adhesive strip will be an elastica by this definition. However, in the last cases treated, the relationship between the bending moment and curvature will be nonlinear, but the strip may still be referred to as an elastica.

2.2 Computer Model

The model for this problem is solved numerically using the computer program Mathematica. A series of programs have been written using the shooting method. The shooting method is a numerical method, in which certain values are known and other values are unknown. Guesses are made for some of the unknown values, while the program solves for the others. Taking the initial guesses and known values, the program

shoots towards an answer that will solve the system of equations. Many times the program would shoot toward the "wrong" answer, illustrating how there are sometimes multiple solutions to the problem, but there is only one that will correctly solve the problem from a physical point of view, and be consistent with the compiled data.

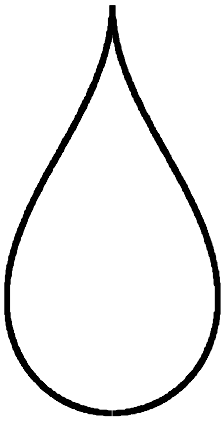

Figure 2.1. Teardrop Shaped Elastica

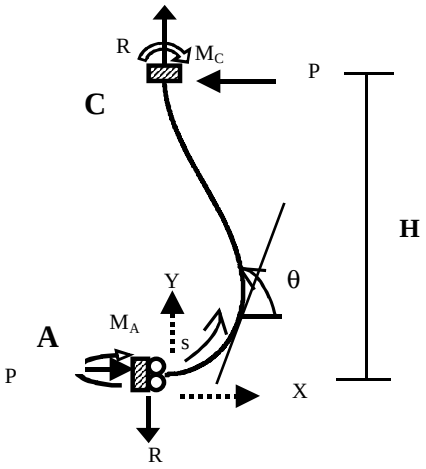

Figure 2.2. Half of Elastica to be Analyzed

Described here is the original formulation of the model; modifications will be mentioned as changes are made in the program. In Figure 2.1 the loop is shown in its initial configuration. Due to the symmetry of the loop, it is possible to analyze half of the loop as shown in Figure 2.2. The variables that are listed in the figure stand for the following:

R represents the equal and opposite vertical forces that act on the half of loop in the middle position;

M_A is the moment at A, at the bottom of the loop;

M_C is the moment at C, at the top of the loop;

P is the horizontal force acting on the loop;

H is the total height of the elastica);

S is the arc length;

θ_B is the angle of the elastica tangent with the horizontal at what is termed point B, which is the point of separation between the elastica and the substrate;

X, Y are the horizontal and vertical coordinates, respectively

The dimensional equations governing the system are as follows:

$$\frac{dX}{dS} = \cos\theta \qquad \frac{dY}{dS} = \sin\theta$$

$$EI\frac{d\theta}{dS} = M \qquad \frac{dM}{dS} = -P\sin\theta - R\cos\theta \qquad \textbf{(2.1-2.4)}$$

E is the modulus of elasticity and I is the moment of inertia of the cross section. In creating this model, the values were nondimensionalized so that the units would not be involved. All following descriptions and figures are in terms of nondimensional quantities. These quantities are as follows:

$$s = \frac{S}{L}, x = \frac{X}{L}, y = \frac{Y}{L}, p = \frac{PL^2}{EI}, r = \frac{RL^2}{EI}, m = \frac{ML}{EI}, h = \frac{H}{L}, m_A = \frac{M_A L}{EI}, m_C = \frac{M_C L}{EI} \qquad \textbf{(2.5-2.13)}$$

After nondimensionalizing each variable, the equations that define the problem are as follows:

$$\frac{dx}{ds} = \cos\theta \qquad \frac{dy}{ds} = \sin\theta \qquad \textbf{(2.14-2.17)}$$

$$\frac{d\theta}{ds} = m \qquad \frac{dm}{ds} = -p\sin\theta - r\cos\theta$$

2.3 Overview of Test Cases

From this foundation, several formulations of the original problem create the work and analysis for the bulk of this thesis. These cases are put forth here as an overview of the cases that will be further explained as the body of the thesis continues.

2.3.1 First Example – Point Contact

The first case verified that the program was working and that the expected results were achievable. This first example portrays the loop right before debonding from the substrate. Here the loop has only a single point of contact (in profile) left to release before the loop tack test would be finished in the pulling part of the cycle. As shown in Figure 2.3, the loop is acted upon by one force with an equal and opposite reaction. This force is termed 2r, and acts at the center of the loop.

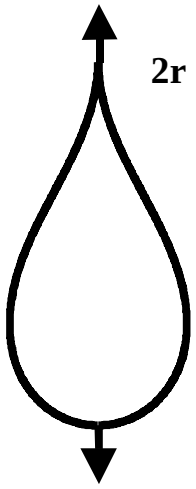

Figure 2.3. Loop with Point Load Acting

2.3.2 Second Example – Flat Contact

While in the initial stages of the computer analysis, experimental work on the loop tack test in the laboratory displayed the loop's configuration throughout the entire testing cycle. During this experiment, it became apparent that the first model of the loop was too round because the elastica in the laboratory experienced a localized curvature near the peel front, and became almost triangular in shape during the pulling phase of the cycle. With this in mind, the second formulation of this problem was created. This was a formulation, in the computer model, which seemed to emulate the pattern set by the lab specimens. This example changed from the first one in that now instead of having the vertical reaction, 2r, acting directly in the center of the

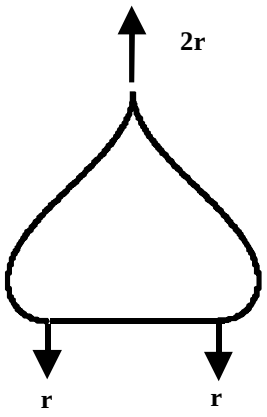

Figure 2.4. Teardrop Shape with Contact Length

loop, it is separated into two individual forces, r, acting a specified contact length, 2b, apart, as seen in Figure 2.4.

2.3.3 Third Example - Pushing and Pulling

Even though the loop was now achieving a triangular shape, it still followed the trends of its predecessor and did not achieve the results that were shown in the laboratory experiments. Therefore, the next formulation for the experiment abandoned the forced triangulation of the second example. This third example changed two factors of the programs that were analyzed by Mathematica. The first of these is that now the adhesive was no longer seen as being on the outside of the elastica, but the adhesive was analyzed as being on the substrate, with the backing pushing into the adhesive mass. This is an equivalent analysis to having the adhesive on the loop, as shown in Figures 2.5 and 2.6.

The second change that took place with the third formulation was that the analysis now included the whole cycle of the loop tack test. Previously, the other two examples included only pulling the elastica from the substrate. Now the loop experiences both the pushing into the substrate and then pulling up from it.

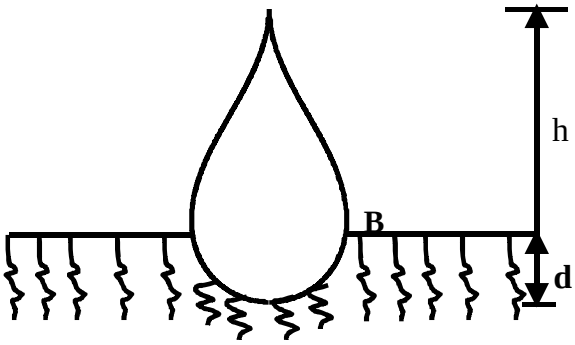

Figure 2.5. Loop with Idealized Foundation

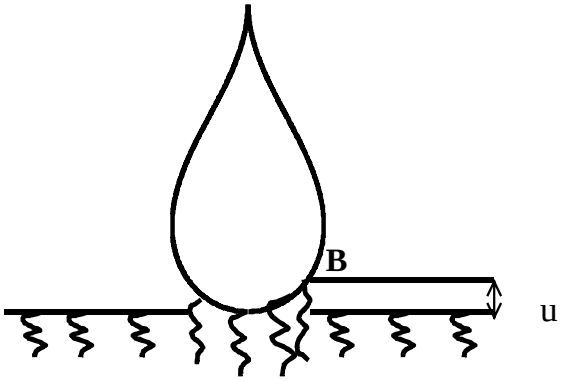

Figure 2.6. Loop Pulling up From Foundation

2.3.4 Fourth Example – Adding Contact Time Dependence

The fourth and last formulation that will be covered in this thesis is a further extrapolation of the third example. This example looks at the elastica in the same way as the previous one but is more realistic, because it takes the adhesive's time of contact with the substrate into account. This creates a system in which the longer the adhesive is in

contact with the substrate, the harder it should be to remove that part of the loop from the substrate.

Each of these components models a specific characteristic of the loop tack test. Each method of looking at the problem develops its own solutions and trends that will give better insight into understanding the behavior of the backing and adhesive during the loop tack test.

Chapter 3

Point Contact

Figure 3.1 illustrates the basis for the first example. The model duplicates the loop tack cycle right before the loop leaves the substrate, because it is in this time frame where the tack force may be at its peak value. As given in chapter two, the first example follows the nondimensionalizing equations numbered 2.5 through 2.13, and also adheres to the preliminary shooting method equations 2.14 through 2.17. In addition, there are a few boundary conditions that constrain the loop's behavior and they are as follows:

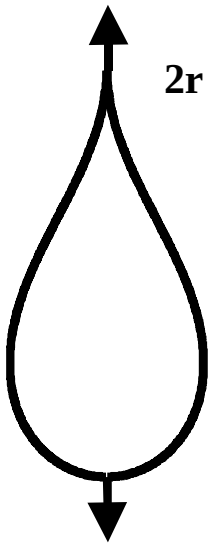

Figure 3.1. Loop with Point Load Acting

At s=0: x=0, y=0, θ=0, m=m_A (unknown).

At s=1: x=0, y=h (unknown), $\theta=\pi/2$, m=m_C (unknown)

These boundary conditions ensure that the loop will maintain the proper configuration during the running of the computer model. This represents the loop's restraints during the actual lab test, where it is held in the jaws of the tensile tester or whatever machine is testing the loop. As mentioned before, it is obvious when the program shoots towards the wrong answer because the graph produced violates the boundary conditions, causing the loop to lose the proper orientation.

3.1 Shooting Method

All of the boundary conditions listed above followed by "unknown" in the parentheses are values the program will determine. In this example, r is a pre-determined value that represents the force acting on the loop. As r increases, the force acting on the loop increases. The values entered for p and m_A are guesses. With the initial guesses and the predetermined values, the program solves for the actual values, which in most cases differ from the initial guesses. The solution for the unloaded configuration, r=0, is known from previous research (Plaut et al., 1999), and is used as the guess for the first

run of the program. The value that is given as the answer, by the computer program, can then be used as the initial guess for the next entered r value. This process continues until the program will no longer solve using the previous answer as the next guess. Once this option for guessing becomes ineffective, certain steps must be taken to make guesses. One method of guessing was to use an extrapolation program that would estimate the next value. If that option did not work, then the next step was to formulate guesses according to the current numerical trends the data was following. For this example, the program computed the values of p, m_A, m_C, h, x_{max}, w, which is 2 x_{max}, and the loop's shapes.

Starting with an r value of zero, the program was run until it was too difficult to generate numbers, which occurred at an r value of 151. As the r value increase the loop becomes taller and narrower. With modifications to the program it may be possible to continue the investigation, but the available data gives no indication of a debonding point, meaning that this analysis could be approaching infinity. In order to give an idea of the type of data that the program returns, Table 3.1 lists a sample of the data returned for the beginning and ending values of r.

Table 3. 1 – Sample Data from First Example

r	p	m_A	h	m_C	w
0	9.91181	5.38413	0.848616	-3.02719	0.408428
151	21.3843	18.6489	0.95325	-1.7356	0.176947

3.2 Results

The graphs that were generated from the collected data display the program's responses within the computer model. Figure 3.2 is a graph of height, h, versus pulling force, r. This graph proves that as the loop's vertical pulling force increases, the loop's height continues to increase as well. This result is expected and illustrates that the program is following the predicted trend. The graph seems to anticipate more results, in that it looks as though it is at the point where it is coming to a plateau, and

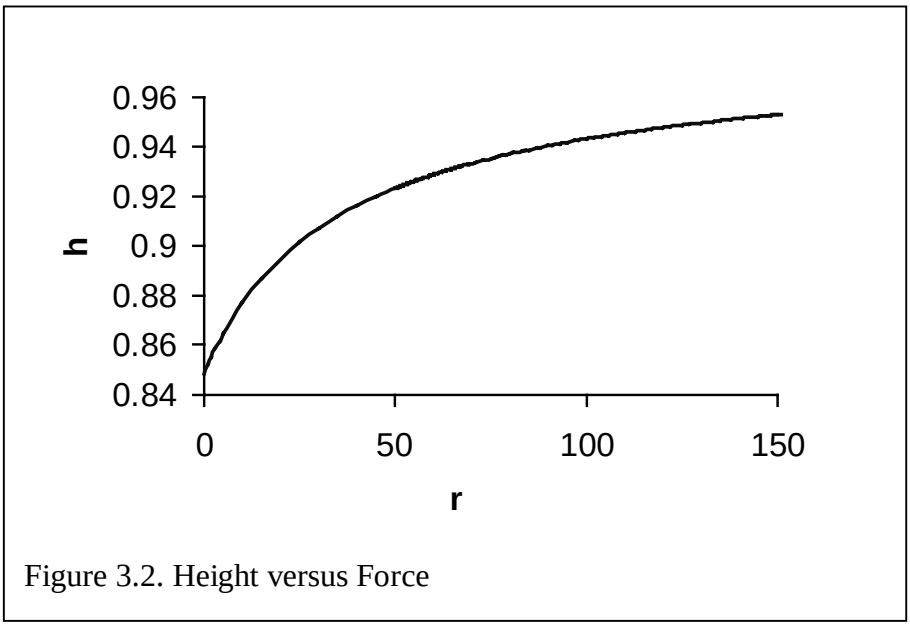

Figure 3.2. Height versus Force

gives no indication of a debonding point, showing that as h is asymptotically approaching one, the r value is approaching infinity.

Figure 3.3 is a graph of the negative moment at point C, at the top of the loop, m_C, versus the force, r. It shows that the moment decreases in magnitude, indicating that this region of the loop is experiencing less moment as it is being pulled upward. This makes sense because at point C, at the top of the loop, the tape should become straighter, because it is being pulled up and the loop is becoming narrower.

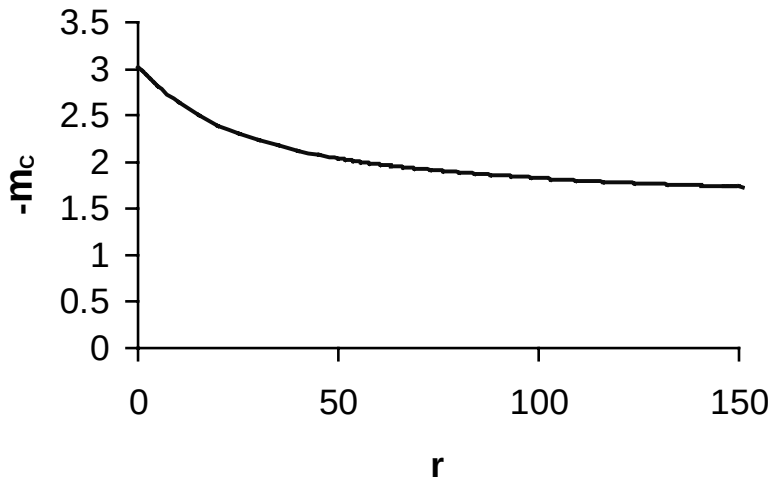

Figure 3.3. Bending Moment at Point C versus Force

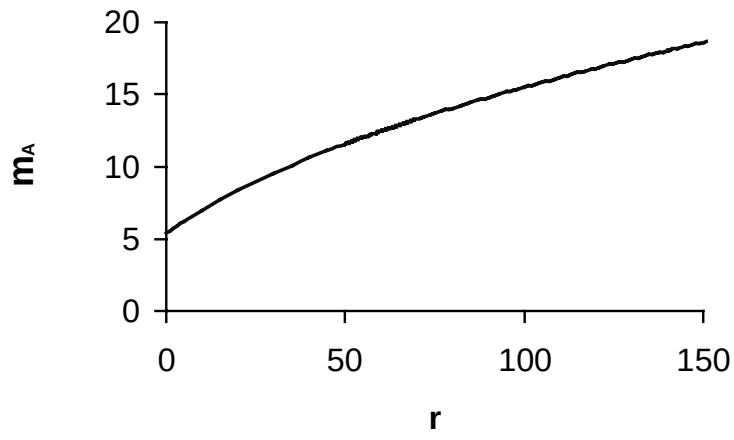

Figure 3.4. Bending Moment at A versus Force

Figure 3.4 is a graph of the bending moment at A, m_A, versus force, r. Unlike the previous graphs, this graph shows an increase in the absolute value of the moment at point A, at the bottom of the loop. As the bottom of the loop achieves a higher curvature, the moment there increases. From equation 2.16, it is known that moment is proportional to the curvature. Due to this fact, curvature increases as the force is increased, meaning that the moment at A increases.

Figure 3.5 shows the width, w, versus the force, r, where w is the total nondimensional width of the elastica that is in contact with the substrate. This graph indicates that the total width of the loop touching the substrate is decreasing as the loop is being pulled upward. This is expected and is consistent with the first graph, Figure 3.2, because as the loop is being pulled up it becomes taller, which would indicate that less of its length should be in contact with the substrate in the actual loop tack test.

Figure 3.6 is a graph of horizontal force, p, versus vertical force, r. This graph shows that as the vertical force r increases, so does the horizontal force, p. This indicates how the loop is pushing against itself. As the horizontal force increases, it gives an indication that the loop is coming closer together and is changing shape.

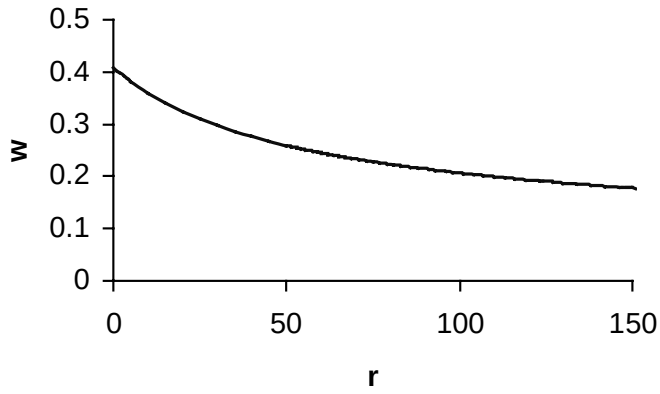

Figure 3.5. Total Width versus Force

Each of these graphs gives an indication of a value that is important in the development of this computer model. Thus far, the trends that were anticipated are shown by the current data. As the analysis continues, it will be observed whether or not this trend continues.

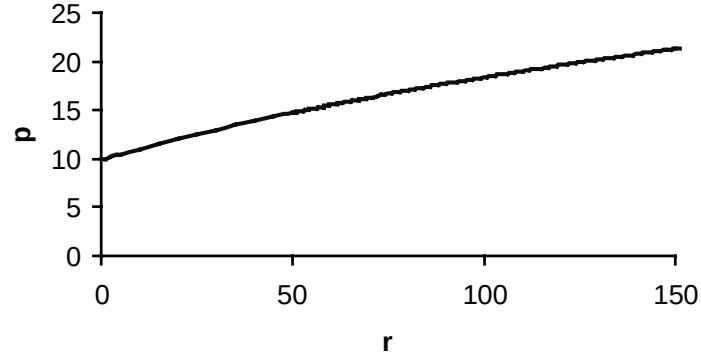

Figure 3.6 – Horizontal Force versus Vertical Force

In addition to these graphs, the loop shapes that Mathematica generates as a part of its analysis are also of interest. Like the graphs, the shapes in Figures 3.7 through 3.10 illustrate the different stages that the loop experiences as it is pulled upward. These diagrams are helpful in visualizing how the loop changes throughout the pulling process.

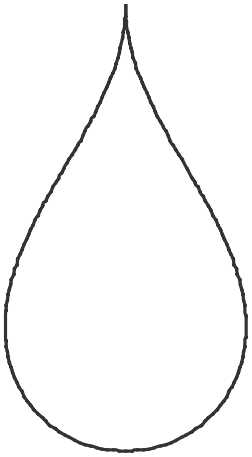

Figure 3.7. Loop with r = 0

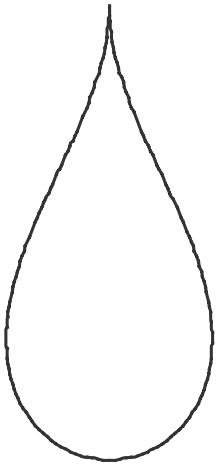

Figure 3.8. Loop with r = 25

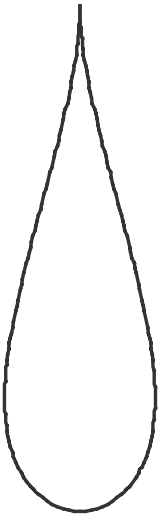

Figure 3.9. Loop with r = 50

Figure 3.10. Loop with r = 100

3.3 Transition

Like the laboratory testing that was conducted, it can be seen that these shapes do follow the expected trends as a “real” loop would experience under actual experimental conditions. The loop is no longer a floppy teardrop shape, but progresses from this initial shape to a narrower shape that gives the indication that the loop is slowly being pulled from the substrate. Unlike the laboratory results, which exhibited a localized curvature at the peel front, as the loop is pulled from the substrate, these diagrams are rather round. The localized curvature will be accounted for, to some extent, in the next formulation of the problem.

Chapter 4

Flat Contact

Concurrently with the beginning of this computer analysis, there were also laboratory experiments of the loop tack test being conducted. Upon visiting the laboratory and watching several runs of the test, it was observed that the loop experiences localized curvature at the peel fronts as it is being pulled from the substrate, as illustrated in Figure 4.1. Unlike the results coming from the computer, which showed the loop remaining round for the complete process, the experiments showed that the loop achieved a triangular shape during the test. After witnessing the laboratory experiments, an attempt was made to create a model that would allow for the localized curvature seen in the actual lab experiments.

Figure 4.1. Loop Pulling Up From Substrate

The new variable that is introduced in this part of the analysis is b, which is half of the contact length in nondimensional terms. It is half the distance that the elastica is wetted out on the substrate surface. The contact length now separates the vertical forces acting on the loop, pulling down on the bottom, as shown in Figure 4.2. The loop is assumed to be flat in the contact region.

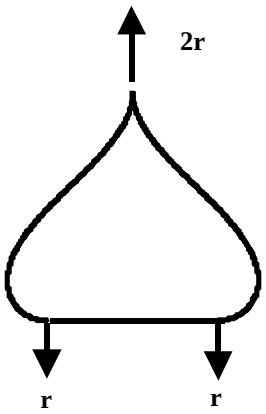

Figure 4.2. Teardrop Shape with Contact Length

4.1 Simple Model of Peeling

An attempt was made to model the high localized curvature by simplifying the system into its most basic parts, as shown in Figure 4.3, in non-dimensional terms. This process will be called the simple peeling procedure and was devised so that an idea of what was happening in the system could be more easily determined.

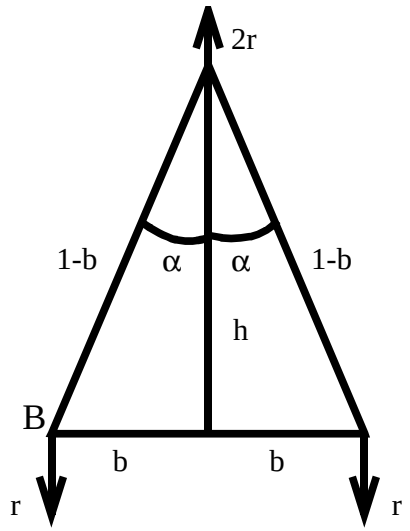

Figure 4.3. Simplified Peeling Model

Since the loop in the lab portrayed a triangular shape during the pulling off portion of the loop tack test, initially it was thought that modeling the loop as a triangle would be a way to better understand what was going on in this particular situation. With the loop as a triangle, it was assumed that the lift-off point, B, moves inward when the horizontal component of the pulling force at that point reaches a certain value J. This value J is the value of the force that causes lift-off at point B. This happens until r reaches an ultimate value of r_U. For this case, and all others, the nondimensional length of the loop is two.

The equations that cover this methodology of analysis include

$$\sin\alpha = \frac{b}{1-b} \qquad \cos\alpha = \frac{h}{1-b}$$

$$\tan\alpha = \frac{b}{h}$$

where $h = \sqrt{1-2b}$ and $b = (1-h^2)/2$ **(4.1-4.3)**

from $b^2 + h^2 = (1\text{-}b)^2$

Point B will move inward when $\frac{rb}{h} = J$ or when

$$\frac{r}{J} = \frac{\sqrt{1-2b}}{b} \qquad \frac{r}{J} = \frac{2h}{1-h^2} \qquad \textbf{(4.4-4.5)}$$

These values can be plotted for the data range of $0 < h < 1$, and $0 < b < 0.5$, as shown in Figures 4.4 and 4.5. Using the data from the laboratory experiments, when the shape is almost triangular, there can be a plot of height, h , versus force, and if that curve looks like the r/J curve, then J can be estimated. Using the Mathematica program there were several graphs that indicate how the r/J graphs should look. This simple model was

abandoned because the two curves that were obtained do not follow the same form, as will be seen in later chapters.

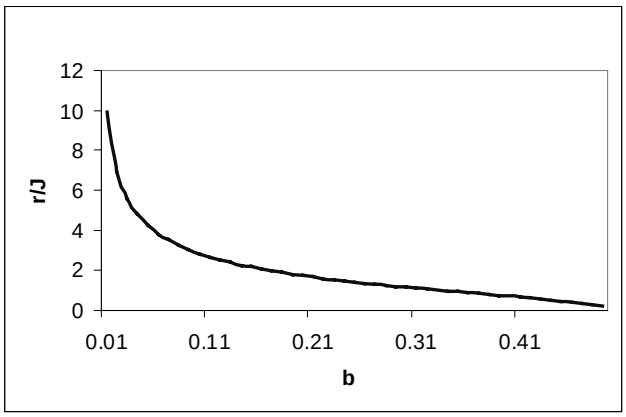

Figure 4.4. Graph of r/J versus Contact Length

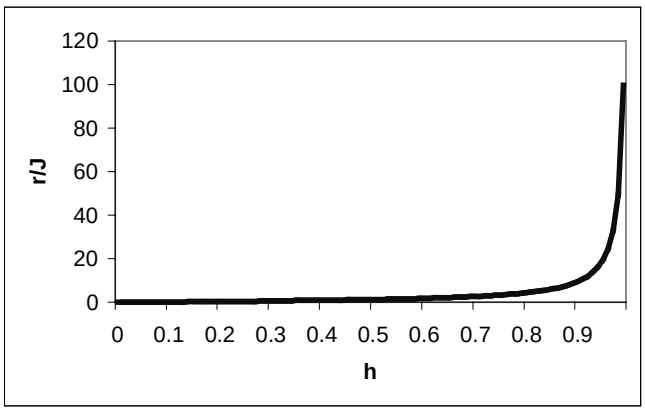

Figure 4.5. Graph of r/J versus Height

4.2 Ramberg-Osgood Model

The next step in moving forward was to create a new type of analysis. Previously, the analysis was simply a linear elastic analysis. From the laboratory experiments, it was observed that the material did not act like a linearly elastic beam, but it was more likely that the material "softened" as the test was being performed. Because of this nonlinearly elastic behavior, the program was modified to try and take the high localized curvature region into effect. This was done by keeping the basics of the model that were discussed in chapter two, and by adding a nonlinear part to the program. This was accomplished with the use of the Ramberg-Osgood nonlinear theory, and relating the curvature to the bending moment as follows:

$$\frac{d\theta}{dS} = \frac{M}{EI_o} + \hat{\beta}\left(\frac{M}{EI_o}\right)^n \qquad \textbf{(4.6)}$$

Here, β and n are positive constants, and EI_o is the initial bending stiffness. The constants can be modified in order to indicate how the material being tested deforms. The quantity EI_o is used to nondimensionalize the rest of the variables that are not lengths, as follows:

$$s=\frac{S}{L}, x=\frac{X}{L}, y=\frac{Y}{L}, p=\frac{PL^2}{EI_o}, r=\frac{RL^2}{EI_o}, m=\frac{ML}{EI_o}, h=\frac{H}{L}, m_A=\frac{M_AL}{EI_o}, m_C=\frac{M_CL}{EI_o} \quad \textbf{(4.7-4.15)}$$

The nondimensional form of $\hat{\beta}$ is

$$\beta=\frac{\hat{\beta}}{L^{n-1}} \quad \textbf{(4.16)}$$

With this in mind, the formula is now

$$\frac{d\theta}{ds}=m+\beta m^n \quad \textbf{(4.17)}$$

where n is greater than one.

Values of β and n were determined by trying to use values that would give an acceptable curve shape. Equation 4.18

$$y = x + \beta x^n \quad \textbf{(4.18)}$$

was plotted in order to verify which values for β and n would be appropriate. Figures 4.6 through 4.9 illustrate the results that were obtained. From these plots it was originally determined that the best values would be n=2 and β=1.5. However, there were some difficulties with this configuration, which created problems within the program and

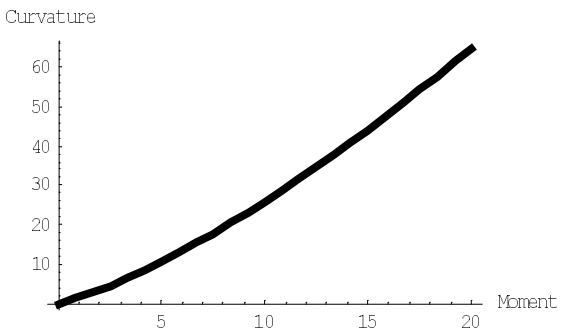

Figure 4.6. Curvature versus Moment for β=0.5 and n= 1.5

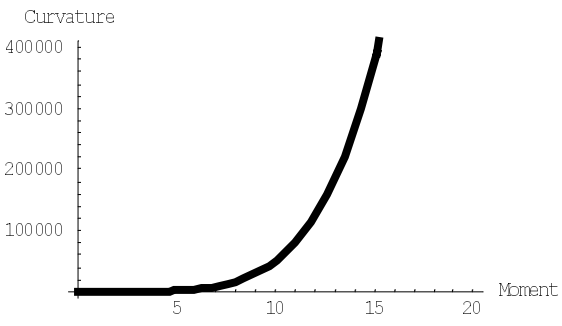

Figure 4.7. Curvature versus Moment for β=0.5 and n= 5

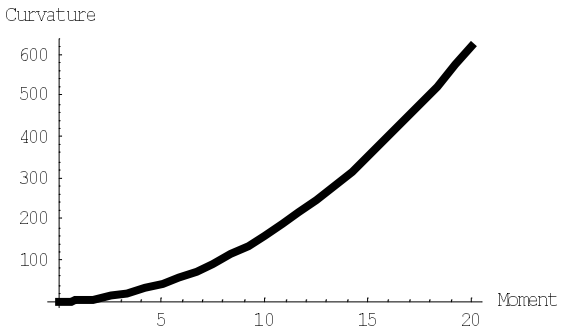

Figure 4.8. Curvature versus Moment for β=1.5 and n= 2

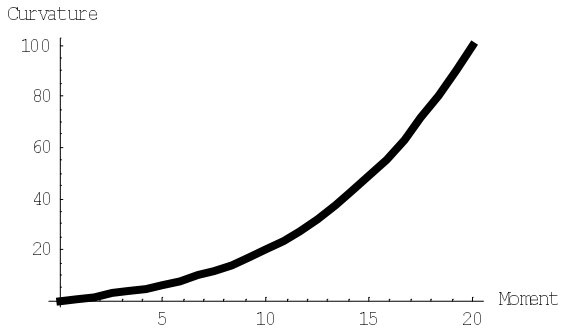

Figure 4.9. Curvature versus Moment for β=0.01 and n=3

prevented it from working properly. Therefore, after several test runs to measure how the program reacted to different numbers, it was decided that the best values to use would be n=3 and β=0.01, which are the values that are used throughout the research.

4.3 Results

Since the modified version of the peel model was unsuccessful, a model similar to the one discussed in Chapter 3 was used. As can be seen in Figure 4.10, this model is very similar to the previous one. The main difference is that now the contact length is taken into account and is specified. It is assumed that the tape in the region of the contact is flat. For a fixed b, values of p and m_B are varied till the conditions at s = 1-b are satisfied with sufficient accuracy. This model is constrained by the following boundary conditions.

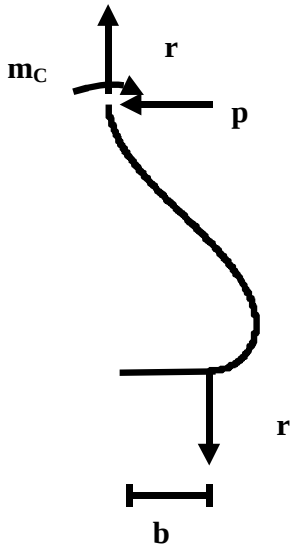

Figure 4.10. Model of Loop System Used in Analysis

At s= 0: $x = 0, y = 0, \theta = 0, m=m_B$

At s=1-b: $x = -b, \theta = \pi/2$

For fixed b, values p and m_B are varied until the conditions at s = 1-b are satisfied with sufficient accuracy. Included are the results for the two cases of b values, b=0.1 and b= 0.2, that were analyzed. Both of these cases follow the same general trend and will be discussed together.

Figures 4.11 and 4.12 plot the graphs for the height, h, versus the force, r. These graphs show the same trend that was experienced in the first example. As the r force increases, the height of the loop increases as well. Once again, as was anticipated, the loop is successfully pulled up from the substrate. What is interesting is that the set of data with

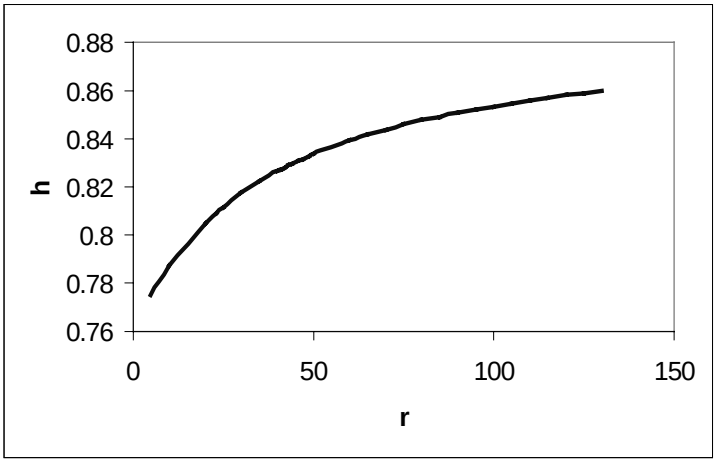

Figure 4.11. Height versus Force, b=0.1

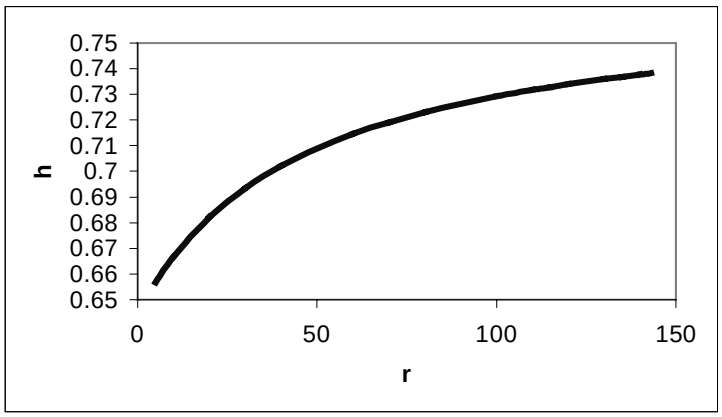

Figure 4.12. Height versus Force, b=0. 2

b= 0.1 is able to achieve a significantly greater height than with b=0.2, most likely because there is less of the elastica's length that is in contact with the substrate for the b = 0.1 case.

Figures 4.13 and 4.14 depict the moment at point B, m_B, versus the force, r, and once again continue the previous trend started in the preceding example. As the r value increases, so does the absolute value of m_B. There may be a number of reasons why the moment at this point increases, but it is most likely because as the tape is pulled up, and the loop is coming closer together, and the moment at the edges is increasing. This would verify that the curvature at the peel fronts would be increasing, since the moment is increasing, causing a greater bending in this area.

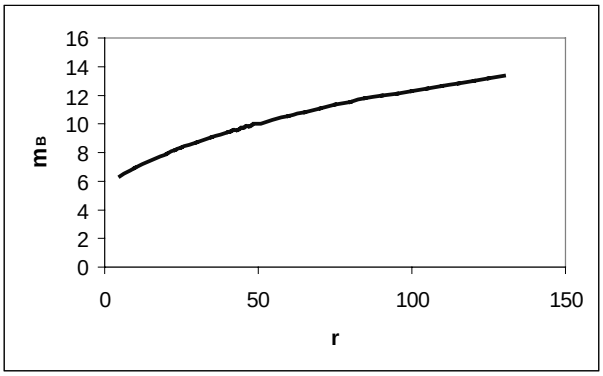

Figure 4.13. Moment at Point B versus Force, b=0.1

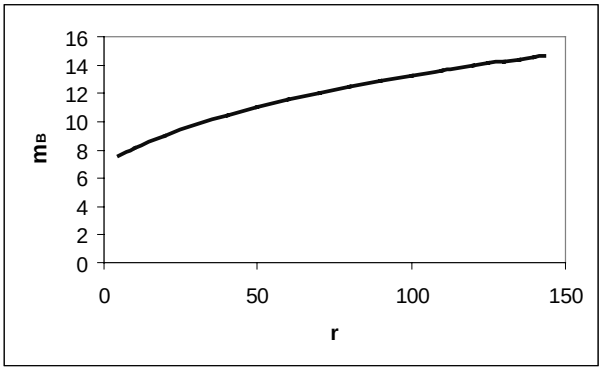

Figure 4.14. Moment at Point B versus Force, b=0.2

Figures 4.14 and 4.15 show the m_C graphs. These graphs are interesting because these graphs appear to be quite different. The graph for b=0.1 seems to follow the same trends as before, in that as r is increasing the m_C magnitude is decreasing; eventually near the higher r values this graph does show an upward trend, which was not seen in the data of chapter 3. The graph corresponding to b = 0.2 does follow the trends set by the other graphs for this same data, but the m_C value begins to increase at a much lower r value. It is uncertain why this occurs. The trend shown in the b = 0.2 graph shows that the moment magnitude at first starts to decrease with the increase in r, but after reaching a certain minimum point, the graph starts to move in the opposite direction. It is possible that this is because of the greater amount of the elastica that is on the substrate. Last of

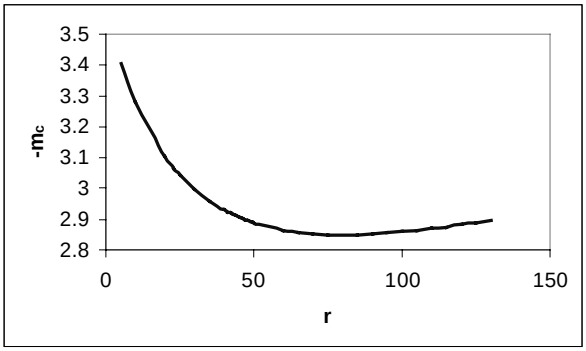

Figure 4.15. Moment at Point C versus Force, b=0.1

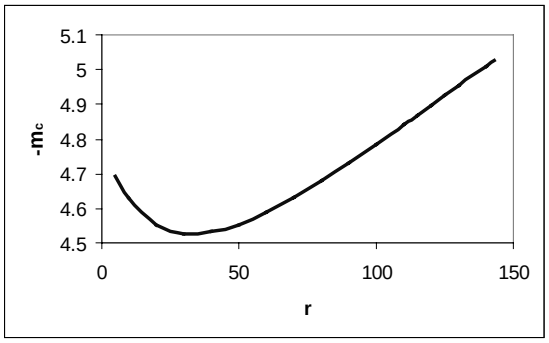

Figure 4.16. Moment at Point C versus Force, b=0.2

all, Figures 4.17 and 4.18 present graphs of the horizontal force, p, versus the vertical force, r. For both the b = 0.1 and 0.2 cases there is the same trend that existed previously. As the r value increases, so does the p value. The curve for b=0.2 has a greater slope than for b=0.1, possibly because the p force experiences a greater change over the same set of r force values.

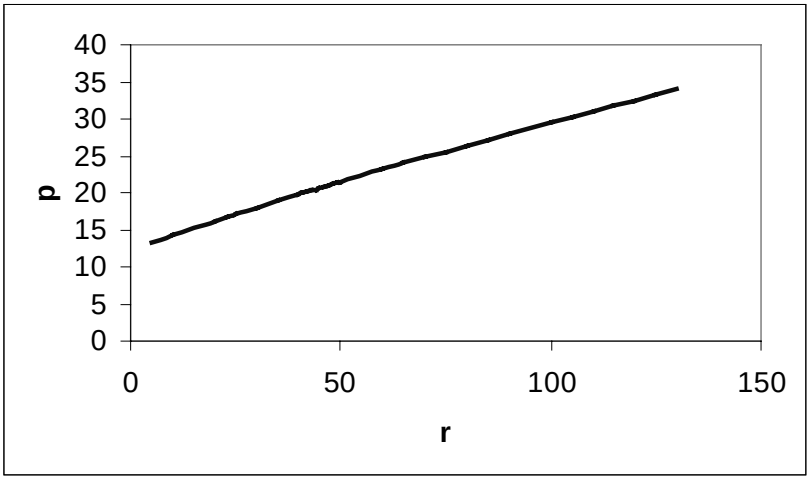

Figure 4.17. Horizontal Force versus Vertical Force, b=0.1

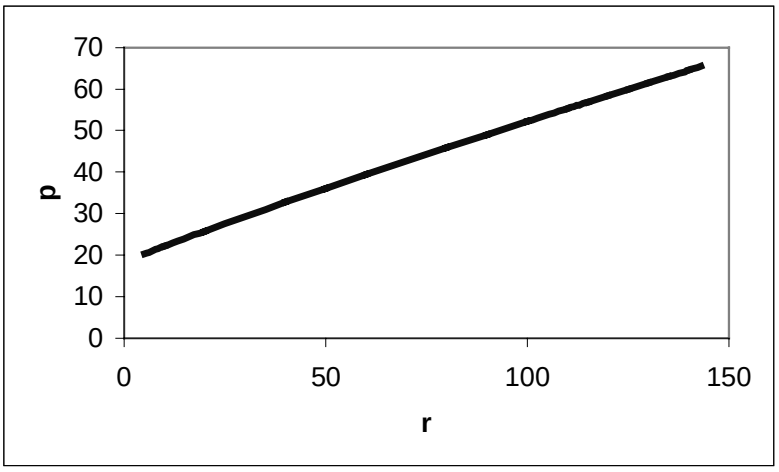

Figure 4.18. Horizontal Force versus Vertical Force, b=0.2

As shown in Figures 4.19 through 4.24, the shapes of the loop display a localized curvature at the lift-off points, as was the goal of this model. However, the figures show that the loops have this localized curvature throughout the duration of the loop tack cycle. This should not occur in practice, because what was observed in the laboratory was a localized curvature near the completion of the loop tack cycle. There is a significant difference between the shapes for the case where b = 0.1 and where b = 0.2. As is noticed through the shapes, the cases with b = 0.1 are taller as they progress throughout the process and these loops also become narrower that the other set, because of the difference in contact length.

4.4 The Next Step

This example did an adequate job of beginning to look at the localized curvature experienced by the system. There are still some issues needing to be addressed, that could not be taken into account with this model. The next model seeks to address the loop tack test as a whole, by looking at both the pushing and pulling parts of the test and by adding some features that will make the analysis more realistic.

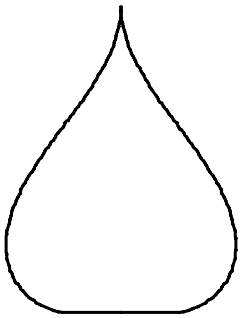

Figure 4.19. Loop with r = 5, b = 0.1

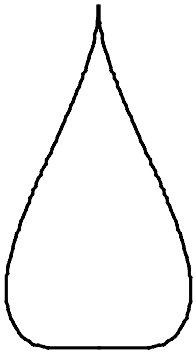

Figure 4.20. Loop with r = 50, b = 0.1

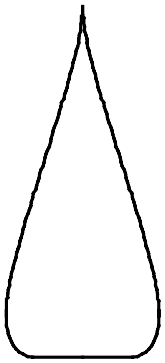

Figure 4.21. Loop with r = 100, b = 0.1

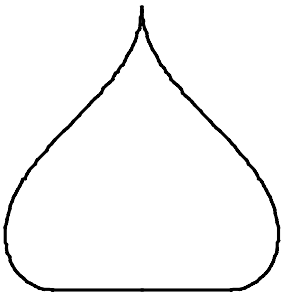

Figure 4.22. Loop with r = 0, b = 0.2

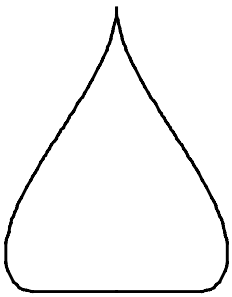

Figure 4.23. Loop with r = 50, b = 0.2

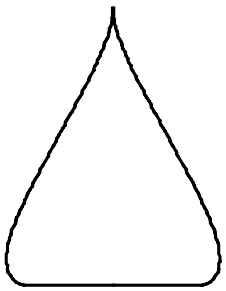

Figure 4.24. Loop with r = 130, b = 0.2

Chapter 5

Pushing and Pulling

5.1 Introduction

The examples that have been looked at thus far have been investigative tools to better understand the behavior of the loop tack test. Both of the previous examples focus on pulling the elastica from the substrate. Now, the complete cycle is observed from beginning to end: pushing into the substrate and then pulling up from the substrate. This analysis is conducted viewing the adhesive as being on the substrate plate, while the backing pushes down into the adhesive mass, an equivalent analysis case to what was used before.

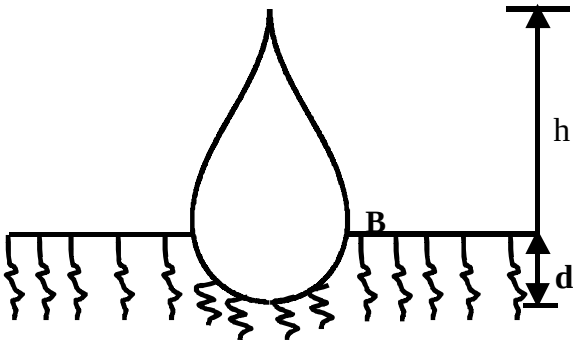

Figure 5.1. Pushing Phase

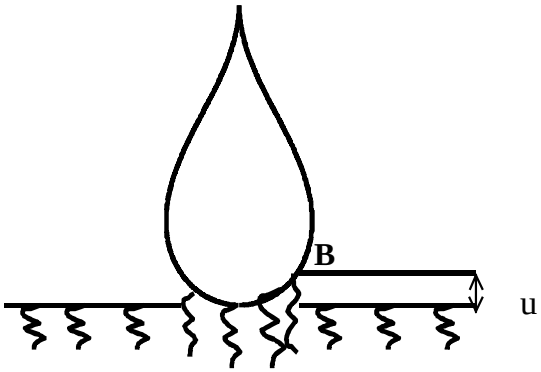

Figure 5.2. Pulling Phase

The nondimensional variables that are introduced in this section of the research are d, u, g, k, s_C, and u_m. These variables are as follows:

d is the distance that the elastica will push down into the adhesive foundation.

u is the distance above the adhesive foundation level to the point where there are no longer any fibril structures hanging onto the elastica, point B.

k represents the relative stiffness of the adhesive and the backing. The dimensional stiffness of the adhesive foundation is denoted K, in units of force per length squared, and k is defined by $k= KL^4/(EI)$, where E is the initial modulus of elasticity of the backing, I is the moment of inertia of its cross section, and L is half the length of the loop. If the cross section has width W and depth H_b, then $I = H_b^3W/12$. Also, if the adhesive has width W, thickness H_a, and modulus of elasticity E_a, then $K=E_aW/H_a$, and k =

$12E_aL^4/(EH_aH_b^3)$. For example, if L = 45 mm, E = 1,000 MPa, H_b = 0.13 mm, H_a = 0.025 mm, and E_a = 0.15 MPa, then k = 1.3 x 10^8. This means that the greater the k value, the less stiff the loop being tested.

Two different k values, k equal to 10^6 and k equal to 10^4, were investigated. Because the k value represents the stiffness of the adhesive and backing, the results from both of these analyses will give an indication of the role that stiffness plays in this test.

s_C is the length of the elastica measured from point B to point C.

u_m represents the maximum deflection experienced for a certain r value.

g is the vertical force in the loop between points A and B, with value g_A at A.

The nonlinear elastic analysis of the Ramberg-Osgood analysis is maintained for this program as well as for the rest of the research.

5.2 The New Model

The loop is divided into two parts. The first is from point A to point B, and the second part of the loop is from point B to point C, as can be seen in Figure 5.3. The bottom part of the loop, from point A to point B, is the part of the loop that is in contact with the foundation. The upper part of the loop, from point B to point C, is the part of the elastica above the foundation. The loop was split because the equations in each section are somewhat different. In the section from A to B, the arc length from B is z, the horizontal axis is ξ, the vertical axis is η, and the angle of the tangent from the horizontal is ϕ, with positive senses shown in Figure 5.3. At B, s = x = y = z = ξ = η = 0 . The equations that govern this formulation of the problem are as follows:

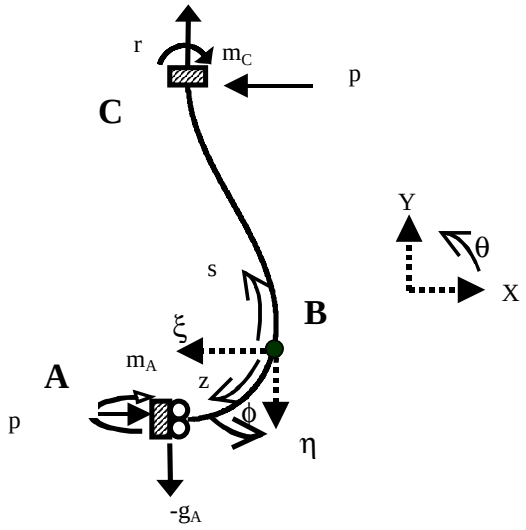

Figure 5.3. Loop Model for this Model Formulation

$$\frac{dx}{ds} = \cos\theta \qquad \frac{dy}{ds} = \sin\theta \qquad \frac{d\theta}{ds} = m + \beta m^3 \qquad \textbf{(5.1-5.3)}$$

$$\frac{dm}{ds} = -p\sin\theta - r\cos\theta \qquad \frac{d\xi}{dz} = \cos\phi \qquad \frac{d\eta}{dz} = \sin\phi$$

$$\frac{d\phi}{dz} = -m - \beta m^3 \qquad \frac{dm}{dz} = p\sin\phi - g\cos\phi \qquad \frac{dg}{dz} = -k\eta$$

(5.4-5.9)

In this formulation b, k, and β are given quantities, while the values p, q, θ_B, m_B, and s_C are each entered as guesses, and will be solved for by the program. Following are the loop's boundary conditions for this problem:

At s=0: x=0; y=0; $\theta=\theta_B$; $m=m_B$

At z =0: ξ=0; η=0; $\phi=\theta_B$; $m=m_B$; g=-r

At $s=s_C$: x=-b; θ=π/2;

At $z=1-s_C$: ξ=b; ϕ=0; g=0

Next, the lengths are scaled to unity using these two equations:

$$\tilde{s} = \frac{s}{s_C} \qquad \tilde{z} = \frac{z}{1 - s_C} \qquad \textbf{(5.10-5.11)}$$

For $0 \le \tilde{s} \le 1$, and $0 \le \tilde{z} \le 1$

$$\frac{d}{ds} = \frac{1}{s_C}\frac{d}{d\tilde{s}} \qquad \frac{d}{dz} = \frac{1}{(1-s_C)}\frac{d}{d\tilde{z}} \qquad \textbf{(5.12-5.13)}$$

and the governing equations are:

$$\frac{dx}{d\tilde{s}} = s_C\cos\theta \qquad \frac{dy}{d\tilde{s}} = s_C\sin\theta \qquad \frac{d\theta}{d\tilde{s}} = s_C(m + \beta m^3)$$

$$\frac{dm}{d\tilde{s}} = s_C(-r\cos\theta - p\sin\theta) \qquad \frac{d\xi}{d\tilde{z}} = (1-s_C)\cos\phi \qquad \frac{d\eta}{d\tilde{z}} = (1-s_C)\sin\phi \qquad \textbf{(5.14-5.22)}$$

$$\frac{d\phi}{d\tilde{z}} = -(1-s_C)(m + \beta m^3) \qquad \frac{dm}{d\tilde{z}} = (1-s_C)(p\sin\phi - g\cos\phi) \qquad \frac{dg}{d\tilde{z}} = -(1-s_C)k\eta$$

Also, $\frac{ds_C}{d\tilde{s}} = 0$ and s_C should be treated as a constant.

The variable that represents both $\tilde{s}$ and $\tilde{z}$ is t in the computer program. In the first five equations

$$t = \frac{s}{s_C} \quad \textbf{(5.23)}$$

and in the other equations

$$t = \frac{z}{1 - s_C} \quad \textbf{(5.24)}$$

The boundary conditions for the example change to the following, now that s and z are represented by t:

At t = 0: x=0, y=0, $\theta=\theta_B$, $m=m_B$, $s_C= s_C$, $\xi=0$, $\eta=0$, $\phi=\theta_B$, $m=m_B$, g=-r

At t = 1: x=-b, $\theta=\pi/2$, $\xi=r$, $\phi=0$, g=0

These equations govern for both the pushing and pulling parts of the model. Adding the numerical factor, u_m distinguishes the pulling part of the model from the pushing. This value u_m is determined by the maximum deflection experienced for a certain b value. Adding u_m makes it so that the pull off condition at point B is dependent on the maximum pressure that was felt at the location during pushing and the previous pulling, and represents the stretched length of the adhesive at which debonding occurs. This pressure creates a resistance of the adhesive so that it is harder to pull the elastica up than it was to push down, and also makes it more difficult to pull up the adhesive as the peel front moves toward the middle. The equation for u_m is assumed to be $u_m=j*\max \eta(b)$, where j is a constant and will be equal to 5. That is, the adhesive is assumed to debond at a location when it reaches a

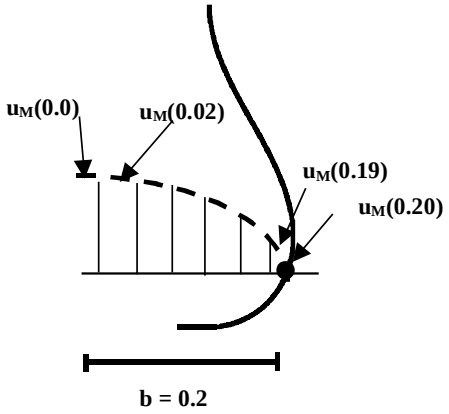

Figure 5.4. Concept of u_m for Debonding

length that is five times the maximum compressed distance (max η) that occurred at that location (see Figure 5.4). Some numerical results are presented in Appendix A.

During pulling, equation 5.22 becomes equation 5.23, in order to indicate pulling, instead of pushing.

$$\frac{dg}{d\tilde{z}} = -k(1-s_C)(\eta - u_m) \quad \textbf{(5.23)}$$

Another equation that was changed is internal to the program, and can be seen in the version of this program in Appendix B.

5.3 Results

The results are now presented for the two cases analyzed, where $k = 10^4$ and $k=10^6$. The results follow the same trends as in previous chapters. The pulling and pushing graphs have been combined, so the whole system can be seen together. The loop was pushed until b=0.2, which corresponds to the maximum achieved in the laboratory experiments where the maximum contact length was 1 inch. The first graphs are those of the force, r, versus the height, h, shown in Figures 5.5 and 5.6. Even though the pushing is included in the graph, there is little change in the trend of the results than what was previously experienced with the other examples. The pushing part is labeled and Figures 5.5 and 5.6 show that as the force is pushing the loop downward (r is decreasing) the height is decreasing. As the force begins to pull in the opposite direction the height of the loop increases, until reaching a peak force value. This is the trend that is expected. In looking at the results for both sets of data, it can be seen that the less stiff elastica ($k = 10^6$) achieves a greater height, probably because there is a greater resistance to keep it on the substrate. The stiffer elastica ($k = 10^4$) does not achieve as high of a height, most likely because the stiffer the elastica, the more likely it is to want to "pop" off from the substrate. The less stiff elastica has a tendency to stay in contact with the substrate longer, which may cause the greater tack value.

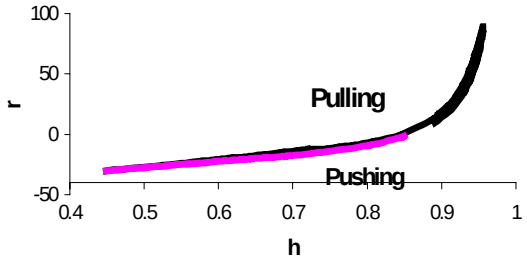

5.5. Force versus Height, k= 10^6

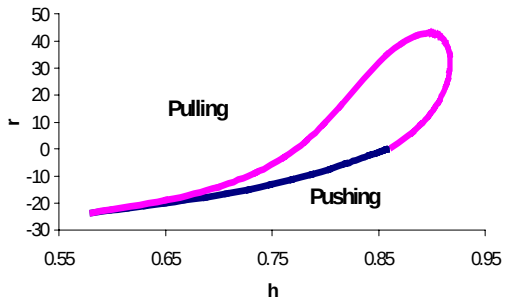

Figure 5.6. Force versus Height, k=10^4

If the vertical force r is controlled, then the loop separates from the substrate at the maximum point of the plot of r versus h. If the vertical deflection at the top of the loop is controlled, then separation occurs when the curve has a vertical tangent (i.e., at the greatest value of h on the curve).

Figures 5.7 and 5.8 are the graphs of the force, r, versus the contact length, b. As was witnessed before, as the force is pushing down, the contact length increases. The contact length goes to b=0.2. As the force begins to pull up, the contact length decreases. These trends are shown in the graph by the curve first going down with the increasing b values and then the graph peaks and then returns to the initial value as the b value decreases, although the loop separates from the substrate before that.

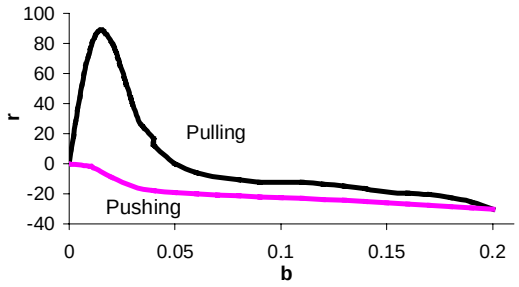

Figure 5.7. Force versus Contact Length, k=10^6

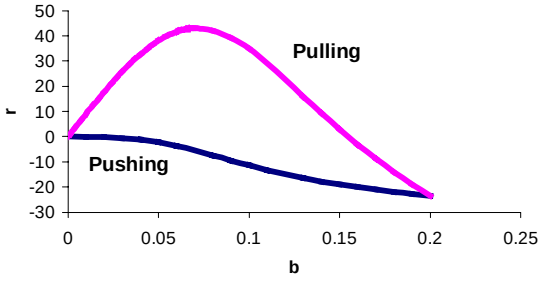

Figure 5.8 Force versus Contact Length, k=10^4

If these experiments were to be conducted in the lab the peak would correspond to the tack. So, it is assumed that the peak shown in the previous Figures 5.5 through 5.8 corresponds to the tack force for the computer generated data. In the lab data it was found, there was often a plateau before this peak. In the computer generated data there is no plateau, and this may be because in the computer analysis there is no fibril structure that is taken into account. In the laboratory experiments the fibril existence may cause the plateau because previous research suggests that fibril formation adds to the tack force (Zosel, 1998) From this data it can also be seen that the elastica with $k = 10^6$ achieves a higher peak force than the one with $k = 10^4$. This would indicate that the greater the relative stiffness of the adhesive, the greater the tack force will be.

There are several other graphs that further show how the system is operating, and the trends that are found within the system. The first is m_B versus b, seen in Figures 5.9 and 5.10. This shows a similar trend for both systems. As the contact length is increasing, the m_B value decreases during the pushing phase of the cycle and then begins to increase as the loop is pulled upward, indicating that less moment is experienced at point B as the loop is pulled upward.

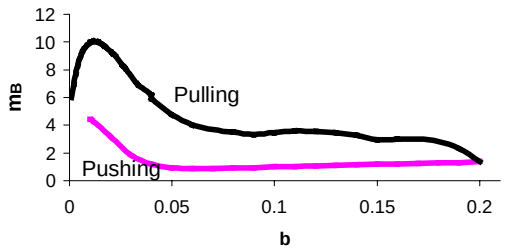

Figure 5.9. Moment at B versus Contact Length, $k = 10^6$

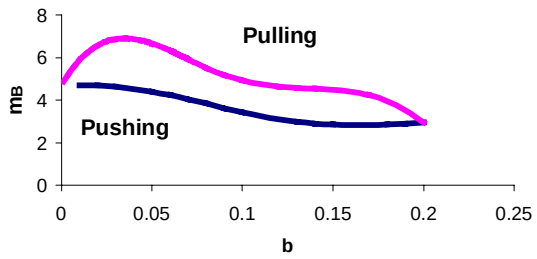

Figure 5.10. Moment at B versus Contact Length, $k = 10^4$

Next, the graph of θ_B versus b, Figures 5.11 and 5.12, shows that as the contact length increases, the angle that is experienced at the lift-off point B increases initially from zero and then decreases for a short time before remaining constant. During pulling the angle increases and after peaking, decreases until returning to the initial value. It is interesting

to note that the angle peaks at quite different values of contact length in the two cases during pulling.

Continuing, Figures 5.13 and Figure 5.14 illustrate the next piece of data in the graphs of the horizontal force, p, versus the contact length, b. These graphs, like many of those before it, show the same trend. As the contact length increases, in the pushing phase, the horizontal force, the p value, decreases and then begins to increase as the pulling phase begins, till there is a maximum point, and then the p value again begins to decrease.

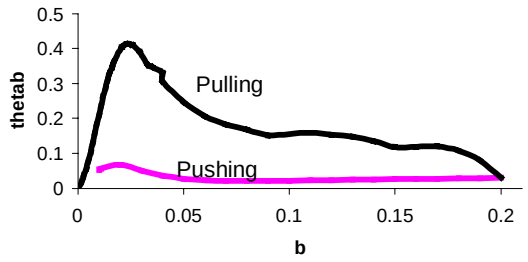

Figure 5.11. Angle at B versus Contact Length, k = 10^6

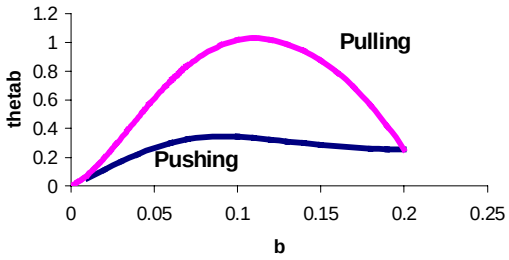

Figure 5.12. Angle at B versus Contact Length, k = 10^4

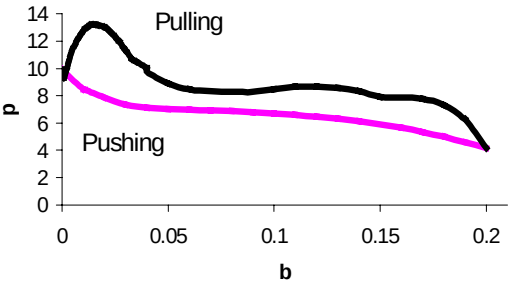

Figure 5.13. Horizontal Force versus Contact Length, k = 10^6

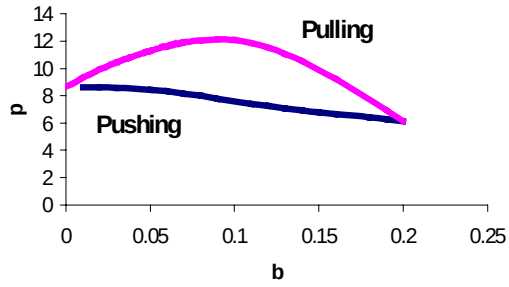

Figure 5.14. Horizontal Force versus Contact Length, k = 10^4

The graph for s_c (the arc length of the part of the loop that is not in contact with the foundation) versus contact length, b, is a straight line, for both pulling and pushing. In the k= 10^4 case there is a slight difference between the two, but for the most part, these

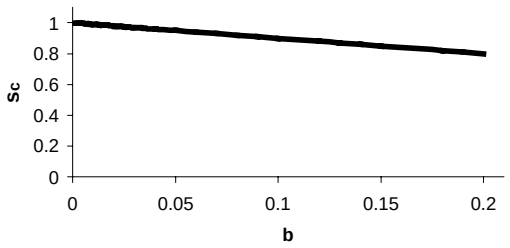

Figure 5.15. Length versus Contact Length, k = 10^6

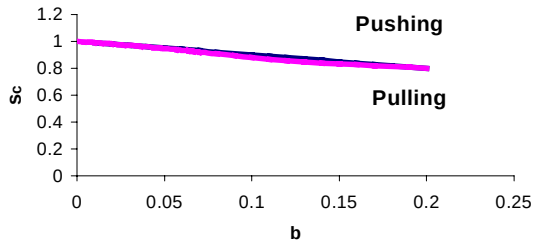

Figure 5.16. Length versus Contact Length, k= 10^4

values are essentially the same for a given contact length.

Figures 5.17 and 5.18 display the graphs of the magnitude of the bending moment at point C, m_C, versus the contact length, b. This trend is different from what the rest of the graphs are experiencing. This is because as the contact length increases, in this case, the value for the magnitude of the moment at point C increases until the peak value is attained, and then as the contact length decreases the value decreases.

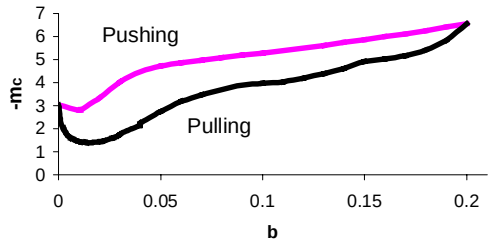

Figure 5.17. Moment at C versus Contact Length, k = 10^6

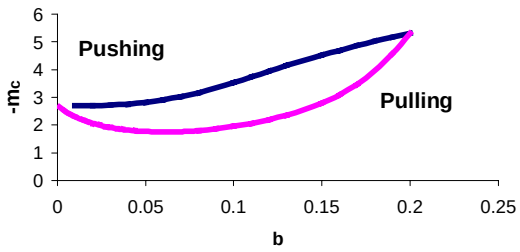

Figure 5.18. Moment at C versus Contac Length, k = 10^4

Another graph that is considered here involves the maximum contact pressure experienced by the loop, determined by multiplying k times the maximum deflection,η. From this graph it can be shown that the pressure experienced is relatively the same at the end of the pushing phase (as b increases to 0.2) and the beginning of the pulling phase (as b decreases from 0.2), but as the elastica is further along in the pulling process, the

pressures continue to increase. This may be an indication of the compressive forces that are at work within this system. Since this pressure is found by looking at the maximum deflection, these graphs suggest that the maximum deflection is experienced as the elastica is being pulled up, which may be contrary to what one might think. This is similar to a peel test: as the top of the loop is pulled upward, part of the loop in contact with the foundation may be pushed further into the foundation.

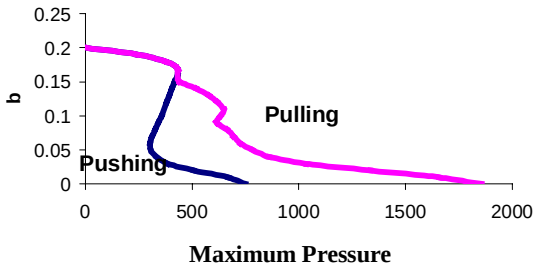

Figure 5.19. Contact Length versus Maximum Pressure, k= 10^6

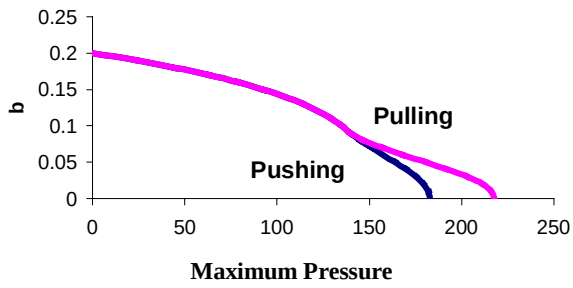

Figure 5.20. Contact Length versus Maximum Pressure, k= 10^4

The computer generated shapes, as they go from pushing to pulling, are shown in Figures 5.21 through 5.28 for the case of k = 10^6 so that one can get an idea of what is going on here. The shapes go through the whole cycle, starting at b=0.01 and running till the maximum contact length value, b =0.2, in Figure 5.24, and then pulling till b = 0.01 (just before the loop separates from the foundation).

5.4 Transition to the Next Chapter

Even though the current program continues to improve in modeling the loop tack test, there are still concerns about points the model does not address. Realizing that the nature of pressure sensitive adhesives leads to viscoelastic behavior, the last model begins to take time effects into account. This will not be a substitute for viscoelastic behavior, but is an initial stepping stone.

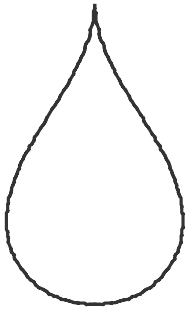

Figure 5.21. b= 0.01

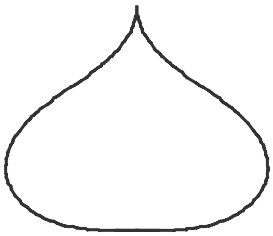

Figure 5.22. b=0.05

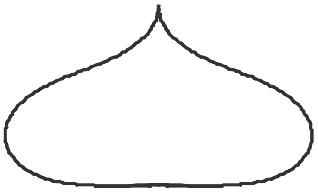

Figure 5.23. b=0.15

Figure 5.24. b= 0.2

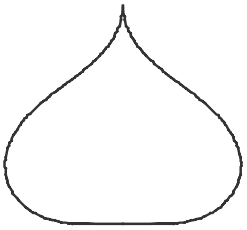

Figure 5.25. b= 0.15

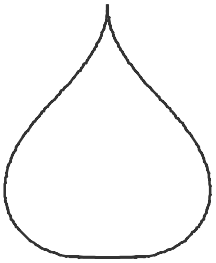

Figure 5.26. b= 0.10

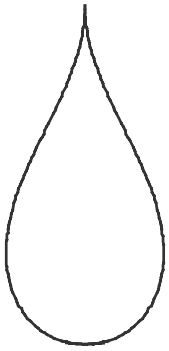

Figure 5.27. b= 0.05

Figure 5.28. b= 0.01

Chapter 6

Addition of Contact-Time Dependence

6.1 Introduction

Chapter five's formulation of the problem accomplished some things that were not being done by the previous examples. Pulling the elastica from the substrate was the focus of the first two examples, while the last example focused on the whole loop tack test cycle. One of the factors that influences the whole process of finding the right formulation is the fact that the adhesive acts like a viscoelastic material. As mentioned previously it is not this research's purpose to account for these viscoelastic effects, but this final example attempts to lay the foundation for the elemental effects of this viscoelastic behavior. For this formulation of the problem, the pushing part of the problem is exactly the same as discussed in chapter five and will not change, but there are changes in the pulling side of the cycle.

6.2 Contact Time

An attempt is made to model the viscoelastic behavior by focusing on the contact time, which is the amount of time the elastica is in contact with the substrate. The basis for the previous example was that as the peel front approaches the center of the loop, the more difficult it should become to remove the elastica from the substrate. Besides the simple position of the peel front, now how long the adhesive has been in contact with the substrate, the contact time, is taken into account. The longer that a piece or section of the adhesive has been in contact with the substrate, the "tougher" it should be to pull that piece of the elastica from the substrate.

6.3 Dependence of Contact Time on Height

Contact time is incorporated by taking advantage of how h, the height, changes with time at a given location. If $\frac{dh}{dt}$ is constant, then the change of |h| is proportional to the contact time, at a given location. In order to determine the contact for a particular b value, all of the heights corresponding to the b value are recorded.

For a given b, the three h values to be considered are:

h_I – height at the initial contact. This is the height of the loop for a particular b value that is recorded during the pushing part of the program.

h_P – height at the end of pushing. This is the height recorded at the end of the pushing cycle. This value is always the same and is the value for b = 0.2.

h_S – height during pulling. This is the height the tape will achieve for a certain b value, as it is being pulled up from the substrate. This value is estimated and put into the program, which then solves for the actual height value. It is assumed that the dwell time between pushing and pulling is zero (or if it is not zero, that its effect is negligible), so;

Δh is the change in $|h|$: $\Delta h = (h_I - h_P) + (h_S - h_P)$, or, $\Delta h = h_I + h_S - 2h_P$. **(6.1)**

The difference in height corresponds to the change in time. The greater the Δh, the more time this section of the elastica has been in contact with the substrate, and should be more difficult to pull off from the substrate. There are a few changes that happen in the body of the program; for those changes, please see Appendix B. The equation for u_m changes to $u_m = (5 + 10\Delta h)\max \eta$. The factor 10 was chosen so that the u_m value is not too small but will make a significant difference now that the height value has been included in its calculation. Thus the stretched length of the adhesive when debonding occurs is assumed to increase linearly with Δh (and thus with the contact time).

6.4 Results

Here again two analyses were studied, one for $k = 10^6$ and the other for $k = 10^4$. Many of these graphs do not return to the original starting point. Because the system is assumed to be elastic, these graphs should come together and meet. Due to the nature of the program, the analysis was ended after reaching a point where the elastica has debonded from the substrate. This point was determined by the height of the elastica decreasing from the maximum height achieved in the analysis. In the laboratory experiments this is where the analysis would have ended, and so these points are not included in the graphs.

The graphs for $k = 10^6$ are incomplete, because data for the graphs at smaller b values was not obtained. There could be several reasons why the program experienced difficulty

in converging to the answers for these points. The nature of the viscoelastic phenomenon that is being taken into account with this model could be causing the barriers found within the program. The data that was obtained is plotted to give a sense of the trends and characteristics for this k value. Figures 6.1 and 6.2 are the graphs for the force r, versus height, h. Once again in this data we see the similar trends. Like the other graphs, this graph shows that as the force acting on the loop increases during pulling, the height of the loop increases as well. Figure 6.1 most closely follows the data that was obtained in the laboratory experiments, please see Appendix C.

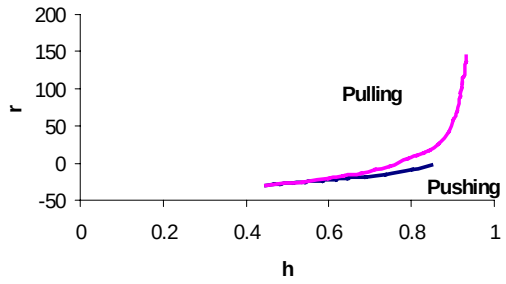

Figure 6.1. Force versus Height, $k=10^6$

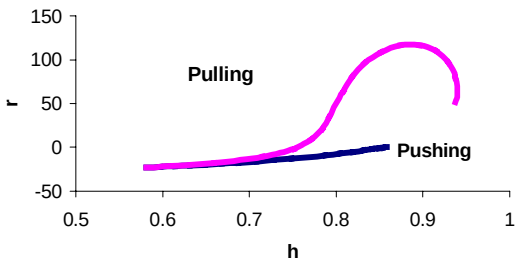

Figure 6.2. Force versus Height, $k=10^4$

Figures 6.3 and 6.4 display the graph of force, r, versus contact length, b. As the force is pushing, the contact length, b, increases. As the force begins to pull up, the contact length decreases.

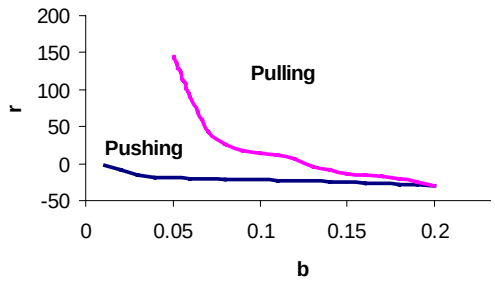

Figure 6.3 Force versus Contact Length, $k = 10^6$

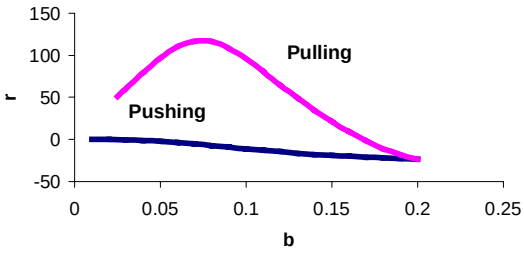

Figure 6.4. Force versus Contact Length, $k=10^4$

Also, Figures 6.5 and 6.6 show the graphs of the angle at point B, θ_B, versus the contact length, b. As the b value increases in pushing, this quantity shows small changes, but as

the pulling part of the program begins, this angle shows increased change as the contact length is decreased. It makes sense that the angle at B should act in this manner, because while pushing, the angle at B does not change greatly. However, once the pulling starts, the angle does change significantly as the loop is pulled upward. This trend is accentuated by the fact that this program intentionally seeks to make it difficult to pull the loop up, and that is why there is such a drastic change in the angle throughout the pulling process.

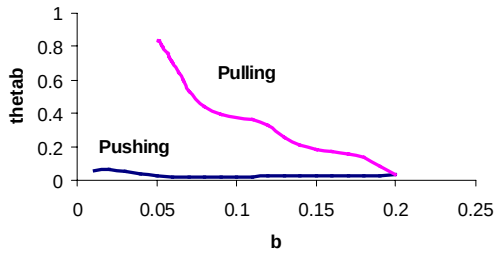

Figure 6.5. Angle at B versus Contact Length, $k=10^6$

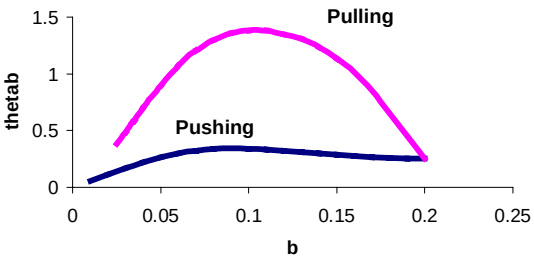

Figure 6.6. Angle at B versus Contact Length, $k=10^4$

The graphs for the horizontal force, p, versus the contact length, b, are shown in Figures 6.7 and 6.8. These graphs show that as the contact length is increasing, the horizontal force, like θ_B, does not exhibit extreme changes, but does decrease. While being pulled up, however, the horizontal force does increase until it peaks, and then begins decreasing again.

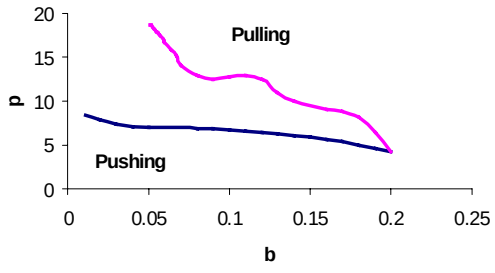

Figure 6.7. Horizontal Force versus Contact Length, $k = 10^6$

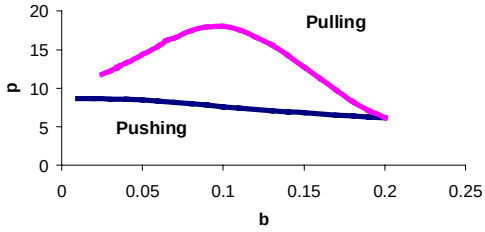

Figure 6.8. Horizontal Force versus Contact Length, $k = 10^4$

Figures 6.9 and 6.10 once again illustrate that s_c is almost the same for pushing and pulling, since it is almost a straight line and it is hard to distinguish between the pushing and pulling sides of the graph. The last two graphs are those for the moment at point B and the moment at point C versus the contact length, b, shown in Figures 6.11 through 6.14. These follow the same trends as before, except the graph of m_B shown in Figure 6.14 has an interesting dip that is unexpected. It is uncertain why the moment at B would change like this and not follow the trends previously witnessed, and begun in Figure 6.13. Figures 6.15 and 6.16 graph the pressure. These graphs are almost identical to those in chapter five; however, these graphs do end at higher pressure values.

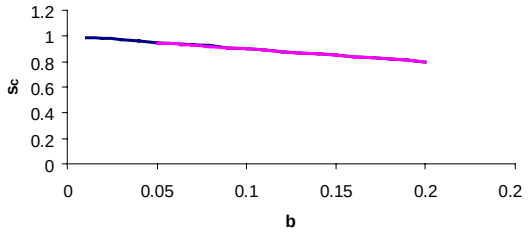

Figure 6.9. Length versus Contact Length, k= 10^6

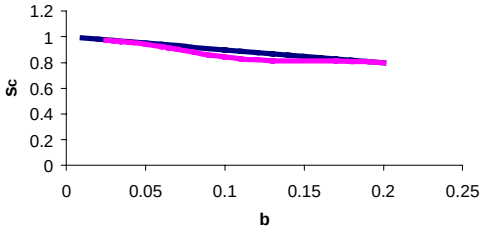

Figure 6.10. Length versus Contact Length, k= 10^4

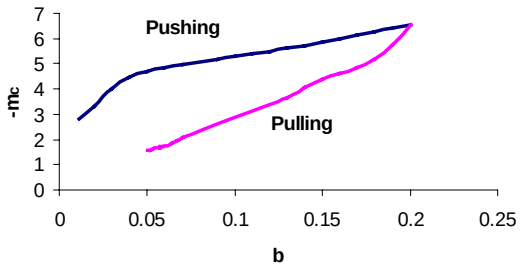

Figure 6.11. Moment at C versus Contact Length, k= 10^6

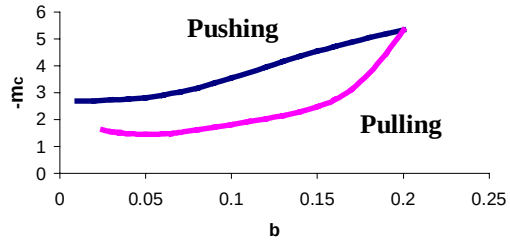

Figure 6.12. Moment at C versus Contact Length, k=10^4

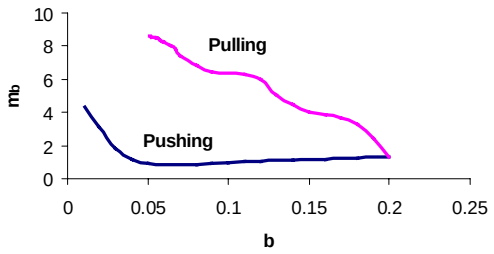

Figure 6.13. Moment at B versus Contact Length, k = 10^6

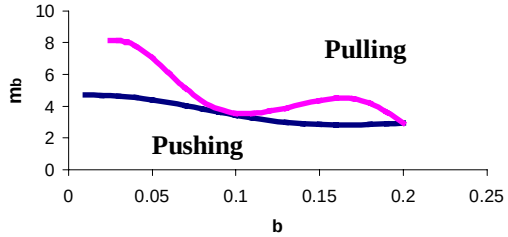

Figure 6.14. Moment at B versus Contact Length, k= 10^4

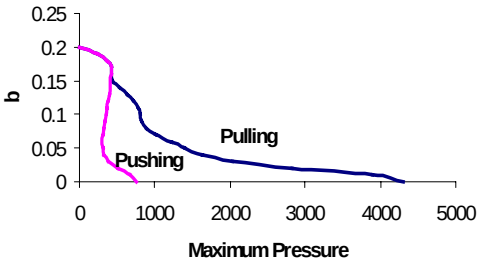

Figure 6.15. Contact Length versus Maximum Pressure, k= 10^6

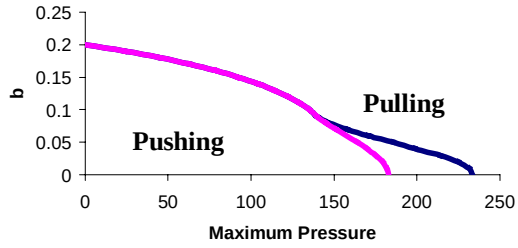

Figure 6.16. Contact Length versus Maximum Pressure, k= 10^4

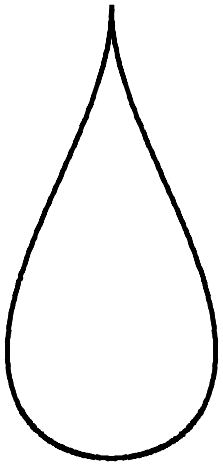

Figure 6.17. b=0.15

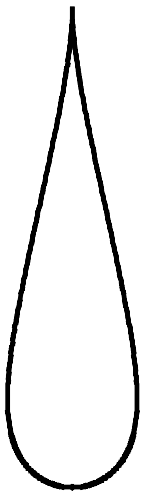

Figure 6.18. b= 0.10

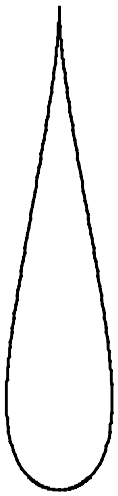

Figure 6.19. b=0.05

Some of the computer generated shapes, for $k = 10^4$, are shown in Figures 6.17 through 6.19 during pulling. These give a general idea of the loop's behavior. The shapes are much taller and narrower than the ones previously generated.

6.5 Comparison Between the Last Two Formulations

Though the last two formulations are not significantly different from each other, in how they are formulated or in how the data is obtained, there are some significant differences that can be seen when some of the graphs are superimposed as far as the values that were achieved for the maximum tack forces. As was previously stated, the pushing part of the system remains the same as that from chapter five to chapter six. The change comes in the pulling side of the graph. Figure 6.20 shows the graph of the force, r, versus height, h. The line labeled chapter five corresponds to the analysis achieved under that system of analysis, and the same is true for the line labeled chapter six. From this graph it can be seen that there is a considerable increase in the maximum tack force that is achieved. The consideration of contact time adds a significant amount to the maximum force the system is able to achieve, based on the criteria for debonding that were assumed here in these two chapters.

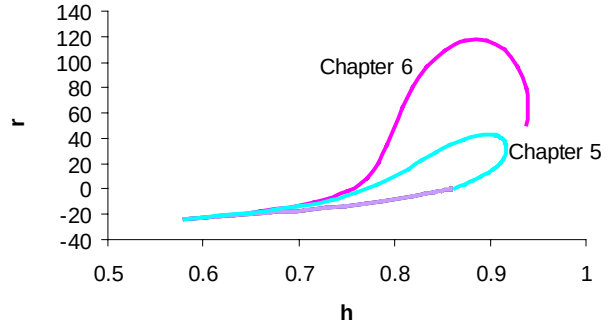

Figure 6.20. Comparison of Force versus Height, $k=10^4$

Also, Figure 6.21 shows another comparison between the results of the two chapters. This figure illustrates the difference in the force achieved against the contact length, b.

Here it is shown that there is a large increase in the peak force that is achieved. It is interesting that the peak force occurs at the same location but in this case is about three times as great in chapter six as that achieved with the analysis in chapter five.

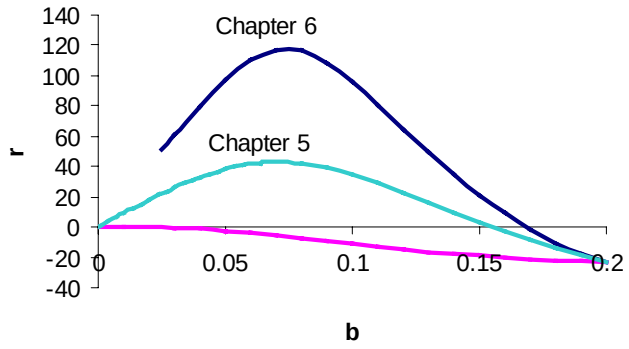

Figure 6.21. Comparison of Force versus Contact Length, k = 10^4

Because the data for k=10^6 is not finished, no visual comparison is shown here. Looking at the figures in this chapter and comparing them with those in chapter five, it can be seen that the graphs do follow similar trends. The graphs created taking the contact time into account, though not finished, are already achieving values significantly greater that the maximums obtained in chapter five.

6.6 Transition to the Conclusions

These are the results that were generated from investigating the loop tack test through a computer analysis instead of in the traditional laboratory methods. There are several conclusions that can be drawn from this research and there are also some things that can be improved. This research also brings up questions and concerns that it could not answer and should be answered in subsequent research studies of other students.

Chapter 7

Conclusions and Recommendations for Future Research

7.1 Summary

This concludes a body of work that seeks to investigate, through an analytical model, the loop tack test and its defining features. Several cases were investigated, using the computer program Mathematica. The beginning models looked at the system being pulled from the substrate. These models were investigative tools used to make sure that the program was working and also to insure that the computer was producing results that would be acceptable as representing results that could be obtained from an actual loop tack test completed in the laboratory. The first example sought to look at the loop right before debonding from the substrate and the behavior it followed. Secondly, in trying to create a more realistic model, it was thought that the high localized curvature that was seen in the laboratory should be included in the computer model, so that the results could be truer to what was observed in the laboratory.

After investigating the pulling up of the elastica from the substrate, the attempt was made to investigate the entire loop tack test cycle. This included first pushing the elastica down onto the substrate and then pulling the elastica from the substrate. In doing this, the essence of the loop tack test and the different events that occur within these pushing and pulling cycles were captured. In seeking to make these models more realistic, a parameter, k, was added which would represent the relative stiffness of the adhesive and backing. The third and fourth example successfully explored what happens during the course of the whole cycle. These examples showed that it was possible to recreate the whole loop tack cycle within the computer. The fourth example also took into account the contact time of the adhesive. This was to help take into account that the longer the adhesive is in contact with the substrate, the more difficult it should be to remove that region of the elastica from the substrate surface. This begins to look at some of the viscoelastic effects that are present and also helps to take into account the fibril action within the system. This formulation seeks to introduce these factors, since these

quantities are crucial to understanding the system's behavior. This was made clear through the results that were achieved, and looking at the comparison between the two sets of data. The fourth example did achieve greater values for the tack force, proving that these characteristics can not be ignored and must be included in future analysis.

7.2 Results

For the most part throughout the data there were several main trends that existed from model to model. The trends that the computer displayed were similar to those trends that were expected from the laboratory results, suggesting that there is reason to pursue this type of research in trying to find alternative methods in the testing and analysis of pressure sensitive adhesives. The research did give an indication of how the system backing and adhesive acted as a whole. The main factors that were shown were that the relative stiffness of the adhesive and backing does matter and does make a difference in the results that are achieved by the loop. This is crucial in determining what sort of backing is used with what type of adhesive. The shapes produced by the analysis gave a realisitic visual representation of the changes caused by the forces acting on the loop during the loop tack test. This research gives the indication that there are many factors involved with pressure sensitive adhesives that affect performance, such as the viscoelastic properties and the debonding criterion.

7.3 Looking Forward

This work lays the foundation for future research, and there are several features that warrant further consideration as research in this area is continued. One of the things that must be considered in future analysis is the time-dependent viscoelastic behavior, and how time plays a crucial role in the procedure. With this also, a further investigation should be made into the importance and significance of the fibril structures that form during the test. The effects of dwell time and loading rate should be studied in the dynamic analysis. Different types of debonding criteria should be considered, with the results compared to those of experimental tests. Plasticity effects in the backing and adhesive could be included. Furthermore, since the deflection of the loop in chapters five and six is not to exceed the thickness of the adhesive, it would be helpful for an analysis to be conducted in which the relative stiffness parameter, k, depends on the amount of

foundation deflection. This k value would approach infinity as the deflection approaches the nondimensional adhesive thickness.

Future research should include finding a way to be more specific about the properties of the elastica. Currently, in the research performed, there is little distinction between the adhesive and the backing, here they work together as a unit. It would be interesting to study how they act together and independently of one another.

Also another area that needs to be explored would be what other sorts of analytical techniques can be used to model this system in the computer. The shooting method works well, but does become rather sensitive in many cases, making it difficult to complete the analysis.

This research proves that there is hope for a computer model that seeks to investigate and model the loop tack test. Ultimately the goal would be to create a program that might one day be successfully incorporated into the testing practices of laboratories.

References

Antman, S. S. and J. F. Pierce (1990). "The Intricate Global Structure of Buckled States of Compressible Columns." *SIAM Journal on Applied Mathematics*, Vol. 50, pp. 395-419.

Aubrey, D.W. (1992). "Pressure-Sensitive Adhesives." Handbook of Adhesion, D.E. Packham, ed., Longman, Essex, UK, pp. 335-341.

Barraclough, P. (1998). "Failure Criteria and Their Application to Visco-elastic/Visco-plastic Materials." Project PAJ1- Interim Report, August.

Chuang, H.K., C. Chiu, and R. Paniagua (1997). "Avery Adhesive Test – A Novel Pressure-Sensitive Adhesive Test Method." Tech XX, 20th Pressure Sensitive Tape Council Proceedings, Boston, Massachusetts, pp. 39-60.

Creton, C. and L. Leibler (1996). "How Does Tack Depend on Time of Contact and Contact Pressure?" *Journal of Polymer Science: Part B: Polymer Physics*, Vol. 34, pp. 545-554.

de Crevoisier, G., P. Fabre, J.-M. Corpart, and L. Leibler (1999). "Switchable Tackiness and Wettability of a Liquid Crystalline Polymer." *Science*, Vol. 285, pp. 1246-1249.

Crosby, A. J. and K. R. Shull (1999). "Adhesive Failure Analysis of Pressure-Sensitive Adhesives." *Journal of Polymer Science: Part B: Polymer Physics*, Vol. 37, pp. 3455-3472.

Dahlquist, C. A. (1982). "Creep." Advances in Pressure Sensitive Adhesive Technology, D. Satas, ed., Satas & Associates, Warwick, RI, pp. 78-83.

Duncan, B.C., L. A. Lay, A. Olusanya, R.A. Roberts, and S. G. Abbott (1999). "The Measurement of Adhesive Tack." Adhesion '99, Seventh International Conference on Adhesion and Adhesives, University of Cambridge, UK, pp. 313-318.

Eppink, D. L. and R. L. Frye (1999). "Adhesives Benchmark Testing." http://www.chemsultants.com.

Fox, R. W. and A. T. McDonald (1992). Introduction to Fluid Mechanics. J. Wiley, New York.

Gay, C. and L. Leibler (1999). "Theory of Tackiness." *Physical Review Letters*, Vol. 82, pp. 936-939.

Goulding, T. M. (1994). "Pressure-Sensitive Adhesives." Handbook of Adhesive Technology, A. Pizzi, K. L. Mittal, eds., Marcel Dekker, New York, pp. 549-564.

References, Continued

Hammond, F. H. Jr. (1982). "Tack." Advances in Pressure Sensitive Adhesive Technology, D. Satas, ed., Satas & Associates, Warwick, RI, pp. 32-49.

Hu, F., A. Olusanya, L.A. Lay, J. Urquhart, and L. Crocker (1998). *A Finite Element Model For the Assessment of Loop Tack for Pressure Sensitive Adhesive Tapes and Labels.* Report 8, Project PAJ1, NPL Report CMMT(B) 129, National Physical Laboratory, Teddington, UK, August.

Johnston, J. (1983a). "Tack – Known by Many Names, It's Difficult to Define." *Adhesives Age*, Vol. 26, pp. 34-38.

Johnston, J. (1983b). "Tack – Probe Testing and the Rate Process." *Adhesives Age*, Vol. 26, pp. 24-28.

Kamagata, K., T. Saito, and M. Toyama (1970). "The Methods of Measuring Tackiness of Pressure Sensitive Adhesive Tapes." *Journal of Adhesion*, Vol. 2, pp. 279-291.

Keimel, F. A. (1994). "Theories and Mechanisms of Adhesion." Handbook of Adhesive Technology, A. Pizzi, K. L. Mittal, eds., Marcel Dekker, New York, pp. 3-15.

Le, M.N., D.A. Dillard, J.G. Dillard and J. Qi (1999). "Analysis of the Loop Tack Test Method for Pressure Sensitive Adhesives." Research Report, Virginia Tech, Blacksburg, VA.

Muny, R. P. (1996). "Getting the Right Results: A Review of PSA Testing Methods." *Adhesives Age*, Vol. 39, pp. 20-24.

Pizzi, A. and K. L. Mittal (1994). Handbook of Adhesive Technology. Marcel Dekker, New York.

Plaut, R. H., S. Suherman, D.A. Dillard, B. E. Williams, and L. T. Watson (1999). "Deflections and Buckling of a Bent Elastica in Contact with a Flat Surface." *International Journal of Solids and Structures*, Vol. 36, pp. 1209-1229.

Pocius, A.V. (1997). Adhesion and Adhesives Technology: an Introduction. Hanser Publishers, New York.

Roberts, R. A. (1997). "Review of Methods for the Measurement of Tack." Report 5, Project PAJ1 – National Physical Laboratory, Teddington, UK, September.

Roberts, R. A. (1999). "Loop Tack Round Robin." Report 10, Project PAJ1 – National Physical Laboratory, Teddington, UK, February.

Russell, T. P. and H. C. Kim (1999). "Tack – a Sticky Subject." *Science*, Vol. 285, pp. 1219-1220.

References, Continued

Satas D., ed. (1989). *Handbook of Pressure- Sensitive Adhesive Technology, 2nd Edition,* van Nostrand, Reinhold Co., New York.

Schultz, J. and M. Nardin (1994). "Theories and Mechanisms of Adhesion." Handbook of Adhesive Technology, A. Pizzi, K. L. Mittal, eds., Marcel Dekker, New York, pp. 19-33.

Zosel, A. (1998). "The Effect of Fibrilation on the Tack of Pressure Sensitive Adhesives." *International Journal of Adhesion and Adhesives,* Vol. 18, pp. 265-271.

Appendix A

In Chapter 5 the concept of u_m was introduced. The equation that describes u_m is $u_m = 5*\max\eta(b)$. This value is a result of the maximum downward deflection that is experienced at a certain contact length value. As the loop was pushed into the foundation, the deflection values were recorded. As the loop was pulled upwards these values were once again recorded. The maximum value for each considered contact length sometimes occurred during the pushing phase; if the pulling deflection happened to be greater, then the η was modified to take this into account. Shown below is an abbreviated version of the chart for $k = 10^6$ for the data collected in chapter five.

Table A. 1

Chart of pushing eta values
All eta values need to be multiplied by 1 E-5

b	0	0.01	0.02	0.03	0.04	0.05	0.06	0.07	0.08	0.09	0.1	0.11	0.12	0.13	0.14	0.15	0.16	0.17	0.18	0.19	0.2
0	0																				
0.01	31	0																			
0.02	68	50.8	0																		
0.03	75	66.9	42.3	0																	
0.04	66	62.4	50.9	30.5	0																
0.05	56	53.8	48.5	38.6	23	0															
0.06	46	45.3	43.2	38.9	31.3	18.9	0														
0.07	37	37.4	37.1	36.1	33.3	27.5	17	0													
0.08	30	30.1	30.9	31.9	32.1	30.6	25.9	16.4	0												
0.09	23	23.2	24.8	26.9	29.1	30.5	29.9	25.8	16.5	0											
0.1	16	17	18.3	21.7	25.1	28.3	30.5	30.4	26.5	17.1	0										
0.11	11	11.5	13.5	16.6	20.6	24.8	28.8	31.4	31.5	27.6	17.8	0									
0.12	6.3	6.94	8.86	11.9	16	20.7	25.5	29.9	32.7	32.9	28.8	18.6	0								
0.13	2.7	3.28	5.02	7.85	11.7	16.3	21.5	26.7	31.2	34.2	34.3	30	19.3	0							
0.14	4.6	5.4	2.02	4.48	7.89	12.2	17.1	22.6	27.9	32.6	35.6	35.7	31.1	20	0						
0.15	-1.8	-1.4	-1.7	1.86	4.74	8.45	13	18.1	23.7	29.2	33.9	36.9	36.9	32.2	20.7	0					
0.16	-2.9	-2.6	-1.6	-5	2.25	5.32	9.18	13.8	19.1	24.7	30.3	35.1	38.2	38.1	33.2	21.3	0				
0.17	-3.4	-3.4	-2.5	-1.4	4.04	2.81	5.95	9.88	14.6	19.9	25.7	31.4	36.3	39.4	39.3	34.2	22	0			
0.18	-3.5	-3.4	-2.9	-2.1	-8.8	9.06	3.33	6.5	10.5	15.2	20.7	26.6	32.4	37.4	40.6	40.5	35.3	22.6	0		
0.19	-3.4	-3.3	-3	-2.5	-1.7	-4.5	1.32	3.75	6.94	11	15.8	21.4	27.4	33.4	38.6	41.8	41.7	36.3	23.3	0	
0.2	-3	-3	-2.8	-2.6	-2.1	-1.3	-0.1	1.6	4.04	7.27	11.4	16.4	22.1	28.3	34.4	39.8	43.1	43	37.4	24	0
Max.	75	66.9	50.8	38.8	33.2	30.5	30.4	31.3	32.7	34.1	35.6	36.9	38.1	39.4	40.6	41.8	43.1	43	37.4	24	0
Press.	750	669	509	389	333	306	305	314	327	342	356	369	382	394	406	418	431	430	374	240	0

Table A.2

Chart of pulling eta values
All eta values need to be multiplied by 1 E-5

b	0	0.01	0.02	0.03	0.04	0.05	0.06	0.07	0.08	0.09	0.1	0.11	0.12	0.13	0.14	0.15	0.16	0.17	0.18	0.19	0.2
0.2	-3	-3	-2.8	-2.6	-2.1	-1.3	-0.1	1.6	4.04	7.27	11.4	16.4	22.1	28.3	34.4	39.8	43.1	43	37.4	24	0
0.19	-4.5	-4.2	-3.3	-1.7	0.72	3.99	8.26	13.6	19.9	27	34.7	42.2	48.6	52.4	51.8	44.3	27	-3.7	-51	-120	
0.18	-3.9	-3.3	-1.5	1.41	5.65	11.2	18.1	26.1	35	44.1	52.7	59.2	61.7	57.9	44.5	17.7	-27	-94	-187		
0.17	-1.2	-3.4	2.14	6.26	12	19.3	27.9	37.5	47.3	56.1	62.7	64.8	59.6	43.7	13.1	-37	-111	-215			
0.16	3.25	4.26	7.27	12.2	19	27.2	36.5	46.1	55	61.4	63.4	58.2	42.3	11.7	-38	-113	-216				
0.15	3.63	4.8	8.26	13.8	21.2	29.9	39.1	47.7	53.9	55.8	50.5	34.7	4.15	-46	-119	-222					
0.14	2.17	23.1	27.3	33.8	42.1	51.2	59.6	65.6	66.4	59	39.4	3.06	-55	-141	-259						
0.13	3.77	39.3	43.6	50.1	57.8	65.1	69.9	69.4	60.2	37.7	-2.7	67	-161	-290							
0.12	5.71	58.4	62.1	67.1	72.2	74.9	72.5	61.1	36.4	-7	-75	-174	-309								
0.11	79.6	80.4	82.3	84.1	83.8	78.4	64.2	36.6	-10	-82	-184	-324									
0.1	99.2	99.1	98	94.5	86.1	69.3	39.8	-7.7	79	-180	-317										
0.09	117	115	110	99.1	79.7	48	-1	-73	-173	-307											
0.08	143	139	126	103	65.7	8.93	-72	-184	-332												
0.07	163	156	133	92.5	29.4	-61	-185	-347													
0.06	178	165	127	60.5	-40	-179	-363														
0.05	185	164	100	-11	-173	-392															
0.04	166	130	20.7	-165	-431																
0.03	66.7	1.24	-195	-517																	
0.02	-25	-361	-668																		
0.01	-722	-830																			
0																					
Max	185	165	133	103	86	78.4	72.4	69.4	66.4	61.4	63.4	64.7	61.7	57.8	51.7	44.3	43.1	43	37.4	24	0
Press.	1856	1659	1335	1034	861	784	725	694	664	614	634	648	617	579	518	443	431	430	374	240	0

Calculations were also made for additional values of b in the range of 0<b<0.03 in increments of 0.001.

From the data listed above, the deflection and the pressure are plotted, to give a better indication of how η changes for varying values of b, as shown in the following graphs.

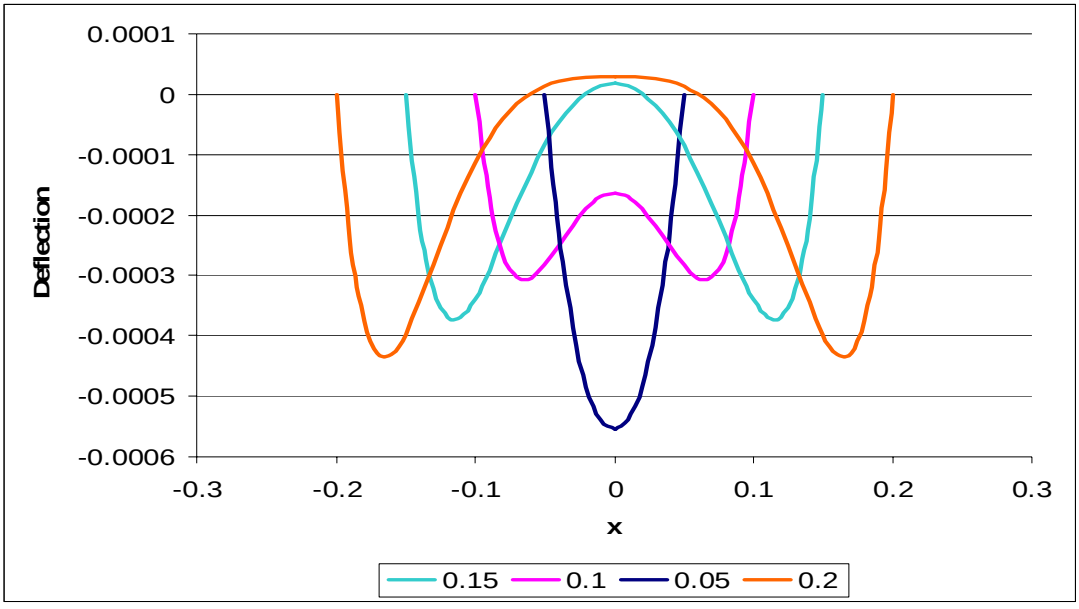

Figure A. 1. Deflection versus Contact Length for Pushing

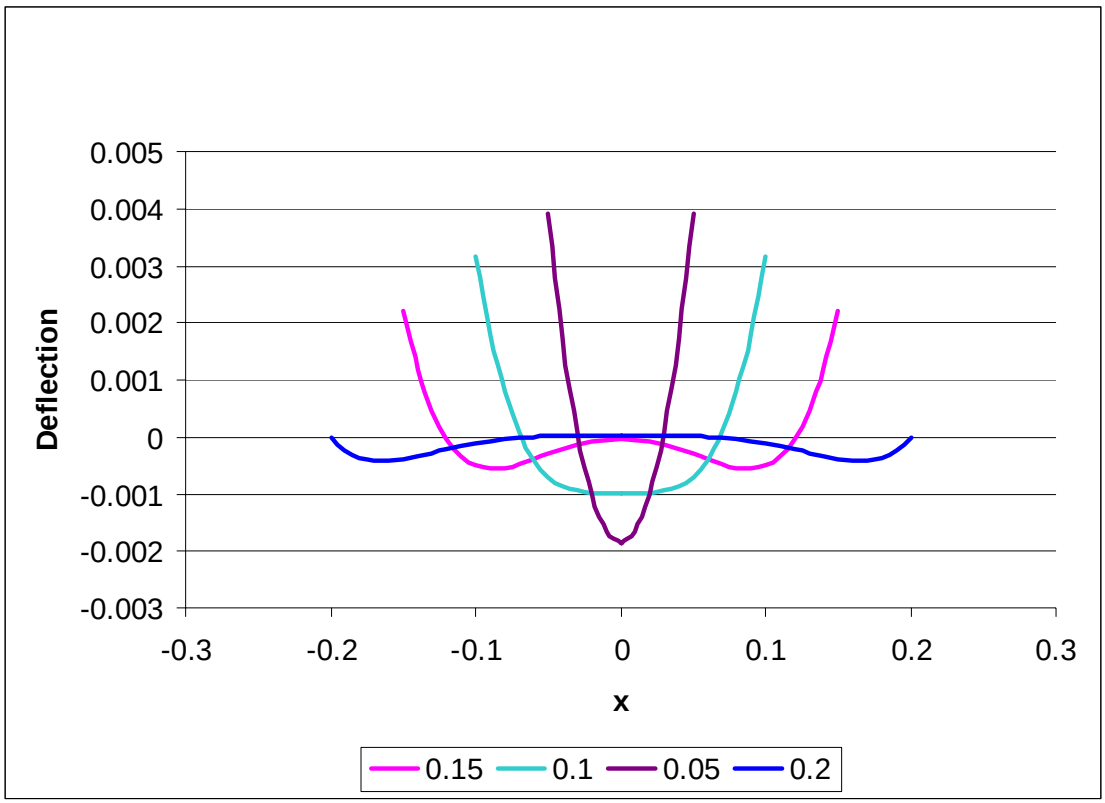

Figure A. 2. Deflection versus Contact Length for Pulling

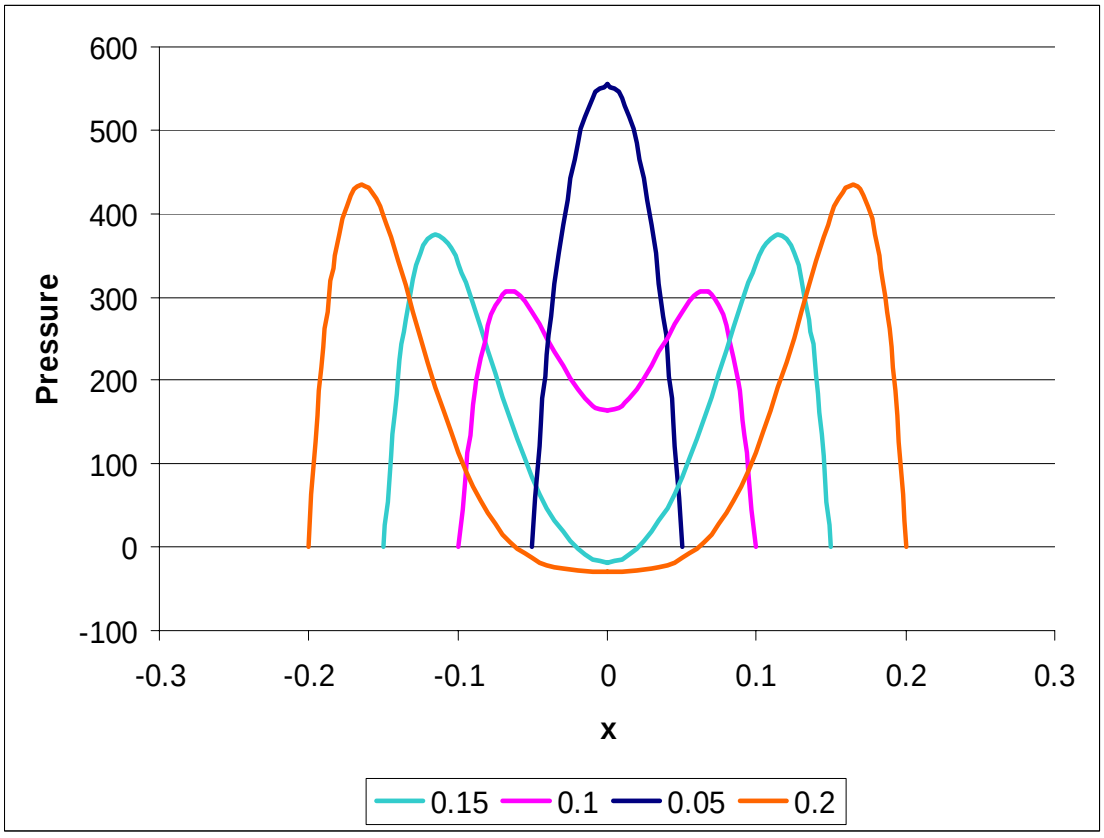

Figure A. 3. Pressure versus Contact Length for Pushing

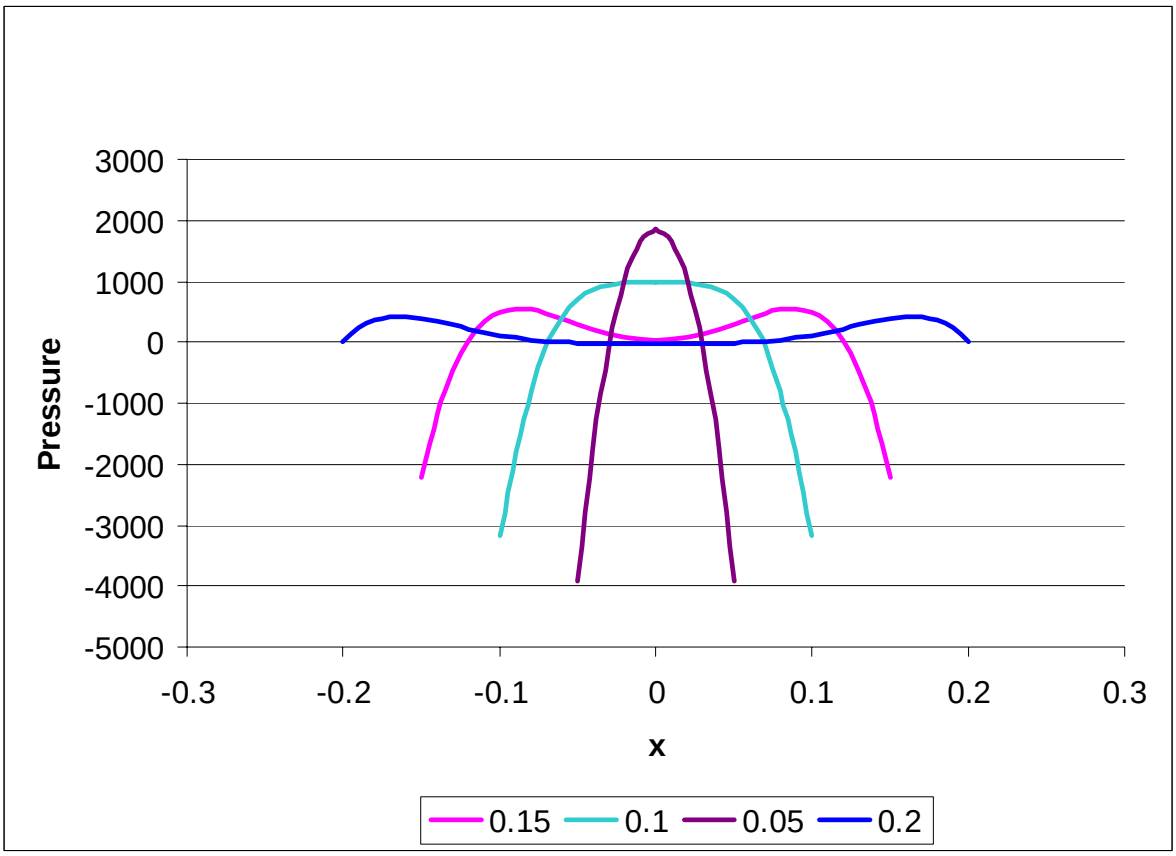

Figure A. 4. Pressure versus Contact Length for Pulling

The horizontal axis in this case is labeled x and the values listed in the legend box correspond to the contact length, or b value, which is the maximum value of x for contact. From the graphs, one can see how the pressure or deflection, in the contact region, for one specific b value, changes as the loop is moving through its cycle of pushing and pulling.

APPENDIX B - *Mathematica* Printouts

Loop Tack Test - Point Contact
Shooting Method to determine variables p (horizontal force) and ma (moment).

Definition of variables:

r = vertical force applied at fixed end of elastica (one side only)
gP = initial guess for parameter P, horizontal force applied at fixed end of elastica
gMA = initial guess for parameter MA, moment existing at center of bent elastica
b = contact length (one half of elastica)

Shooting Method

```
c = 0

r = 0

b = 0

pi = N[π]

gP = 9.91

gMA = 5.38

de[y3_, y4_, P_] := {y1'[t] == Cos[y3[t]], y2'[t] == Sin[y3[t]],
  y3'[t] == y4[t], y4'[t] == -P Sin[y3[t]] - r Cos[y3[t]]}

leftBC[MA_] := {y1[0] == 0, y2[0] == 0, y3[0] == 0, y4[0] == MA}

soln := NDSolve[Flatten[Append[de[y3, y4, P], leftBC[MA]]],
  {y1, y2, y3, y4}, {t, 0, 1 - b}, MaxSteps → 2200]

endpt[P_, MA_] := {y1[t], y2[t], y3[t], y4[t]} /.
    First[NDSolve[Flatten[Append[de[y3, y4, P], leftBC[MA]]],
      {y1[t], y2[t], y3[t], y4[t]}, {t, 0, 1 - b}, MaxSteps → 2200]] /. t -> 1 - b;
endpt[
 gP,
 gMA]

Clear[P, MA]

rts := FindRoot[{endpt[P, MA][[3]] == pi/2, endpt[P, MA][[1]] == c - b},
  {P, {gP, 0.99 gP}}, {MA, {gMA, 0.99 gMA}}, AccuracyGoal → 4, MaxIterations → 200]


rts

endpt[P /. rts, MA /. rts]
```

```
P = P /. rts
            MA = MA /. rts


Print[P /. soln /. rts]
Print[MA /. soln /. rts]

{yy1[t_], yy2[t_], yy3[t_], yy4[t_]} = {y1[t], y2[t], y3[t], y4[t]} /. First[soln]

List[P /. rts, MA /. rts,
 Part[endpt[P /. rts, MA /. rts], 2], Part[endpt[P /. rts, MA /. rts], 4]]

ParametricPlot[Evaluate[{yy1[t], yy2[t]} /. soln /. rts], {t, 0, 1},
 PlotRange -> All, AspectRatio -> Automatic, PlotPoints -> 1000]



numbers = TableForm[
  Table[Evaluate[{yy1[t] /. soln /. rts, yy2[t] /. soln /. rts}], {t, 0, 1, .01}],
  TableHeadings -> {None, {"x", "y"}}]


numb = TableForm[Table[Evaluate[{yy1[t] /. soln /. rts}], {t, 0, 1, .01}],
  TableHeadings -> {None, {"x"}}]


pipe = Max[%]


w = 2 pipe
```

Loop Tack Test - Flat Contact

Shooting Method to determine variables p (horizontal force) and MA (moment).

Definition of variables:

r = vertical force applied at fixed end of elastica (one side only)

gP = initial guess for parameter P, horizontal force applied at fixed end of elastica

gMA = initial guess for parameter MA, moment existing at center of bent elastica

b = contact length (one half of elastica)

Shooting Method

```
r = 5

c = 0

b = 0.1

n = 3

β = 0.01

pi = N[π]

gP = 15.19

gMA = 5.93

de[y3_, y4_, P_] := {y1'[t] == Cos[y3[t]], y2'[t] == Sin[y3[t]],
  y3'[t] == y4[t] + (β * (y4[t]^n)), y4'[t] == -P Sin[y3[t]] - r Cos[y3[t]]}

leftBC[MA_] := {y1[0] == 0, y2[0] == 0, y3[0] == 0, y4[0] == MA}

soln := NDSolve[Flatten[Append[de[y3, y4, P], leftBC[MA]]],
  {y1, y2, y3, y4}, {t, 0, 1 - b}, MaxSteps → 2200]

endpt[P_, MA_] := {y1[t], y2[t], y3[t], y4[t]} /.
    First[NDSolve[Flatten[Append[de[y3, y4, P], leftBC[MA]]],
      {y1[t], y2[t], y3[t], y4[t]}, {t, 0, 1 - b}, MaxSteps → 2200]] /. t -> (1 - b);
endpt[
 gP,
 gMA]

Clear[P, MA]
```

```
rts := FindRoot[{endpt[P, MA][[3]] == pi/2, endpt[P, MA][[1]] == c - b},
  {P, {gP, 0.89 gP}}, {MA, {gMA, 0.89 gMA}}, AccuracyGoal → 4, MaxIterations → 1000]

rts

endpt[P /. rts, MA /. rts]

P = P /. rts
            MA = MA /. rts

Print[P /. soln /. rts]
Print[MA /. soln /. rts]

{yy1[t_], yy2[t_], yy3[t_], yy4[t_]} = {y1[t], y2[t], y3[t], y4[t]} /. First[soln]

Print[yy1[1 - b]]
Print[yy3[1 - b]]

List[P /. rts, MA /. rts,
 Part[endpt[P /. rts, MA /. rts], 2], Part[endpt[P /. rts, MA /. rts], 4]]

ParametricPlot[Evaluate[{yy1[t], yy2[t]} /. soln /. rts], {t, 0, 1 - b},
 PlotRange -> All, AspectRatio -> Automatic, PlotPoints -> 1000]

patterns = TableForm[
  Table[Evaluate[{yy1[t] /. soln /. rts, yy2[t] /. soln /. rts}], {t, 0, (1 - b), .01}],
  TableHeadings -> {None, {"x", "y"}}]

numb = TableForm[Table[Evaluate[{yy1[t] /. soln /. rts}], {t, 0, (1 - b), .01}],
  TableHeadings -> {None, {"x"}}]

pipe = Max[%]

w = 2 pipe

List[P /. rts, MA /. rts, Part[endpt[P /. rts, MA /. rts], 2],
 Part[endpt[P /. rts, MA /. rts], 4], pipe]
```

Loop Tack Test - Pushing Down

Shooting Method to determine variables p (horizontal force), mb (moment), θb(angle), sc(arc length), and q(vertical force).

Definition of variables:

q = vertical force applied at fixed end of elastica (one side only -referred to as r in the thesis body)

gP = initial guess for parameter P, horizontal force applied at fixed end of elastica

gMb = initial guess for parameter Mb, moment existing at peel front of bent elastica

r = contact length (one half of elastica) (referred to as b in the thesis body)

θb = angle at point B on the elastica

sc = arc length

k = relative stiffness

Shooting Method

```
pi = N[Pi, 10]

r = 0.1

gP = 5

gθb = 0.03

gMb = 1.0

gq = 29

gsc = 0.90

k = 1000000

n = 3

B = 0.01

de[y3_, y4_, y5_, y7_, y8_, y9_, y10_, P_, q_] := {y1'[t] == y5[t] * Cos[y3[t]],
  y2'[t] == y5[t] * Sin[y3[t]], y3'[t] == y5[t] * (y4[t] + (B * (y4[t]^n))),
  y4'[t] == y5[t] * ((q * Cos[y3[t]]) - (P * Sin[y3[t]])), y5'[t] == 0,
  y6'[t] == (1 - y5[t]) * Cos[y8[t]], y7'[t] == (1 - y5[t]) * Sin[y8[t]],
  y8'[t] == -(1 - y5[t]) * (y9[t] + (B * (y9[t]^n))),
  y9'[t] == (1 - y5[t]) * ((P * Sin[y8[t]]) - (y10[t] * Cos[y8[t]])),
  y10'[t] == -(1 - y5[t]) * k * y7[t]}

leftBC[θb_, Mb_, sc_, q_] := {y1[0] == 0, y2[0] == 0, y3[0] == θb, y4[0] == Mb,
  y5[0] == sc, y6[0] == 0, y7[0] == 0, y8[0] == θb, y9[0] == -Mb, y10[0] == q}

soln :=
 NDSolve[Flatten[Append[de[y3, y4, y5, y7, y8, y9, y10, P, q], leftBC[θb, Mb, sc, q]]],
  {y1, y2, y3, y4, y5, y6, y7, y8, y9, y10}, {t, 0, 1}, MaxSteps → 2200]
```

```
endpt[P_, Mb_, sc_, eb_, q_] :=
  {y1[t], y2[t], y3[t], y4[t], y5[t], y6[t], y7[t], y8[t], y9[t], y10[t]} /.
    First[NDSolve[Flatten[Append[de[y3, y4, y5, y7, y8, y9, y10, P, q],
        leftBC[eb, Mb, sc, q]]], {y1[t], y2[t], y3[t], y4[t], y5[t], y6[t],
       y7[t], y8[t], y9[t], y10[t]}, {t, 0, 1}, MaxSteps → 2200]] /. t -> 1;
endpt[
 gP,
 gMb,
 gsc,
 geb,
 gq]

Clear[P, Mb, sc, eb, q]

rts := FindRoot[{endpt[P, Mb, sc, eb, q][[3]] == pi/2,
   endpt[P, Mb, sc, eb, q][[1]] == -r, endpt[P, Mb, sc, eb, q][[6]] == r,
   endpt[P, Mb, sc, eb, q][[8]] == 0, endpt[P, Mb, sc, eb, q][[10]] == 0},
  {P, {gP, 0.99 gP}}, {Mb, {gMb, 0.99 gMb}}, {sc, {gsc, 0.99 gsc}},
  {eb, {geb, 0.99 geb}}, {q, {gq, 0.99 gq}}, AccuracyGoal → 10, MaxIterations → 200]


rts

endpt[P /. rts, Mb /. rts, sc /. rts, eb /. rts, q /. rts]


P = P /. rts
            Mb = Mb /. rts
sc = sc /. rts
eb = eb /. rts
q = q /. rts

Print[P /. soln /. rts]
Print[Mb /. soln /. rts]

Print[sc /. soln /. rts]

Print[eb /. soln /. rts]

Print[q /. soln /. rts]

{yy1[t_], yy2[t_], yy3[t_], yy4[t_],
  yy5[t_], yy6[t_], yy7[t_], yy8[t_], yy9[t_], yy10[t_]} =
 {y1[t], y2[t], y3[t], y4[t], y5[t], y6[t], y7[t], y8[t], y9[t], y10[t]} /. First[soln]

List[P /. rts, Mb /. rts, sc /. rts, eb /. rts, q /. rts,
 Part[endpt[P /. rts, Mb /. rts, sc /. rts, eb /. rts, q /. rts], 2],
 Part[endpt[P /. rts, Mb /. rts, sc /. rts, eb /. rts, q /. rts], 4]]
```

```
numbers = TableForm[
  Table [{k, P /. soln /. rts, Mb /. soln /. rts, sc /. soln /. rts, eb /. soln /. rts,
    q /. soln /. rts, Part[endpt[P /. rts, Mb /. rts, sc /. rts, eb /. rts, q /. rts], 2],
    Part[endpt[P /. rts, Mb /. rts, sc /. rts, eb /. rts, q /. rts], 4]}, {u, u, u}],
  TableHeadings → {None, {"k", "P", "Mb", "sc", "eb", "q", "h", "Mc"}}]


bok2 = ParametricPlot[Evaluate[{yy1[t], yy2[t]} /. soln /. rts],
  {t, 0, 1}, PlotRange -> All, AspectRatio -> Automatic, PlotPoints -> 3000,
  GridLines -> Automatic, PlotStyle -> {{Thickness[0.02]}}]



bok3 = ParametricPlot[Evaluate[{(r - yy6[t]), -(yy7[t])} /. soln /. rts],
  {t, 0, 1}, PlotRange -> All, PlotPoints -> 3000,
  GridLines -> Automatic, PlotStyle -> {{Thickness[0.02]}}]



patterns = TableForm[
  Table[Evaluate[{yy1[t] /. soln /. rts, yy2[t] /. soln /. rts}], {t, 0, 1, .01}],
  TableHeadings -> {None, {"x", "y"}}]


patte = TableForm[
  Table[Evaluate[{(r - yy6[t]) /. soln /. rts, -(yy7[t]) /. soln /. rts}], {t, 0, 1, .01}],
  TableHeadings -> {None, {"6", "7"}}]


patter = TableForm[Table[Evaluate[{yy1[t] /. soln /. rts}], {t, 0, 1, .1}],
  TableHeadings -> {None, {"x"}}]



lemon = Max[%]

w = 2 lemon


lily = (Part[endpt[P /. rts, d /. rts], 2] - d)

TableForm[
 Table[{t, Evaluate[yy1[t]], Evaluate[yy2[t]], Evaluate[yy3[t]], Evaluate[yy4[t]]},
  {t, 0, 1, .01}], TableHeadings -> {None, {"t", "xb", "yb", "e", "Mb"}}]

numbers = TableForm[Table [
   {k, xb, P /. soln /. rts, d /. soln /. rts, Part[endpt[P /. rts, d /. rts], 2], lily},
   {u, u, u}], TableHeadings → {None, {"k", "xb", "P", "d", "h", "hu"}}]


Print[w]
```

```
chat = TableForm[Table[Evaluate[{yy7[y/(100*r)] /. soln /. rts}], {y, 0, (r*100), 1}],
  TableHeadings -> {None, {"y7"}}]

cha = TableForm[Table[Evaluate[{(yy6[1] - yy6[y/(100*r)]) /. soln /. rts}],
   {y, 0, (r*100), 1}], TableHeadings -> {None, {"y6"}}]
```

Loop Tack Test - Pulling Up

Shooting Method to determine variables p (horizontal force), mb (moment), θb(angle), sc(arc length), and q(vertical force).

Definition of variables:

q = vertical force applied at fixed end of elastica (one side only -referred to as r in the thesis body)

gP = initial guess for parameter P, horizontal force applied at fixed end of elastica

gMb = initial guess for parameter Mb, moment existing at peel front of bent elastica

r = contact length (one half of elastica) (referred to as b in the thesis body)

um = represents the maximum downward deflection

θb = angle at point B on the elastica

sc = arc length

k = relative stiffness

Shooting Method

```
pi = N[Pi, 10]

r = 0.2

maxη = 0.0004312

um = 5 * maxη

gP = 4.1448

gθb = 0.030375

gMb = 1.3461

gq = 30.18315

gsc = 0.7999

k = 1000000

n = 3

B = 0.01
```

```
de[y3_, y4_, y5_, y7_, y8_, y9_, y10_, P_, q_] := {y1'[t] == y5[t] * Cos[y3[t]],
  y2'[t] == y5[t] * Sin[y3[t]], y3'[t] == y5[t] * (y4[t] + (B * (y4[t]^n))),
  y4'[t] == y5[t] * ((q * Cos[y3[t]]) - (P * Sin[y3[t]])), y5'[t] == 0,
  y6'[t] == (1 - y5[t]) * Cos[y8[t]], y7'[t] == (1 - y5[t]) * Sin[y8[t]],
  y8'[t] == -(1 - y5[t]) * (y9[t] + (B * (y9[t]^n))),
  y9'[t] == (1 - y5[t]) * ((P * Sin[y8[t]]) - (y10[t] * Cos[y8[t]])),
  y10'[t] == -(1 - y5[t]) * k * (y7[t] - um)}

leftBC[eb_, Mb_, sc_, q_] := {y1[0] == 0, y2[0] == 0, y3[0] == eb, y4[0] == Mb,
  y5[0] == sc, y6[0] == 0, y7[0] == 0, y8[0] == eb, y9[0] == Mb, y10[0] == q}

soln :=
 NDSolve[Flatten[Append[de[y3, y4, y5, y7, y8, y9, y10, P, q], leftBC[eb, Mb, sc, q]]],
  {y1, y2, y3, y4, y5, y6, y7, y8, y9, y10}, {t, 0, 1}, MaxSteps → 2200]

endpt[P_, Mb_, sc_, eb_, q_] :=
  {y1[t], y2[t], y3[t], y4[t], y5[t], y6[t], y7[t], y8[t], y9[t], y10[t]} /.
    First[NDSolve[Flatten[Append[de[y3, y4, y5, y7, y8, y9, y10, P, q],
        leftBC[eb, Mb, sc, q]]], {y1[t], y2[t], y3[t], y4[t], y5[t], y6[t],
      y7[t], y8[t], y9[t], y10[t]}, {t, 0, 1}, MaxSteps → 2200]] /. t -> 1;
endpt[
 gP,
 gMb,
 gsc,
 geb,
 gq]

Clear[P, Mb, sc, eb, q]

rts := FindRoot[{endpt[P, Mb, sc, eb, q][[3]] == pi/2,
   endpt[P, Mb, sc, eb, q][[1]] == -r, endpt[P, Mb, sc, eb, q][[6]] == r,
   endpt[P, Mb, sc, eb, q][[8]] == 0, endpt[P, Mb, sc, eb, q][[10]] == 0},
  {P, {gP, 0.99 gP}}, {Mb, {gMb, 0.99 gMb}}, {sc, {gsc, 0.99 gsc}},
  {eb, {geb, 0.99 geb}}, {q, {gq, 0.99 gq}}, AccuracyGoal → 10, MaxIterations → 200]


rts

endpt[P /. rts, Mb /. rts, sc /. rts, eb /. rts, q /. rts]


P = P /. rts
            Mb = Mb /. rts
sc = sc /. rts
eb = eb /. rts
q = q /. rts

Print[P /. soln /. rts]
Print[Mb /. soln /. rts]

Print[sc /. soln /. rts]
```

```
Print[eb /. soln /. rts]

Print[q /. soln /. rts]

{yy1[t_], yy2[t_], yy3[t_], yy4[t_],
  yy5[t_], yy6[t_], yy7[t_], yy8[t_], yy9[t_], yy10[t_]} =
 {y1[t], y2[t], y3[t], y4[t], y5[t], y6[t], y7[t], y8[t], y9[t], y10[t]} /. First[soln]

List[P /. rts, Mb /. rts, sc /. rts, eb /. rts, q /. rts,
 Part[endpt[P /. rts, Mb /. rts, sc /. rts, eb /. rts, q /. rts], 2],
 Part[endpt[P /. rts, Mb /. rts, sc /. rts, eb /. rts, q /. rts], 4]]

numbers = TableForm[
  Table [{k, P /. soln /. rts, Mb /. soln /. rts, sc /. soln /. rts, eb /. soln /. rts,
    q /. soln /. rts, Part[endpt[P /. rts, Mb /. rts, sc /. rts, eb /. rts, q /. rts], 2],
    Part[endpt[P /. rts, Mb /. rts, sc /. rts, eb /. rts, q /. rts], 4]}, {u, u, u}],
  TableHeadings → {None, {"k", "P", "Mb", "sc", "eb", "q", "h", "Mc"}}]


bok2 = ParametricPlot[Evaluate[{yy1[t], yy2[t]} /. soln /. rts],
  {t, 0, 1}, PlotRange -> All, AspectRatio -> Automatic, PlotPoints -> 3000,
  GridLines -> Automatic, PlotStyle -> {{Thickness[0.02]}}]



bok3 = ParametricPlot[Evaluate[{(r - yy6[t]), -(yy7[t])} /. soln /. rts],
  {t, 0, 1}, PlotRange -> All, PlotPoints -> 3000,
  GridLines -> Automatic, PlotStyle -> {{Thickness[0.02]}}]



patterns = TableForm[
  Table[Evaluate[{yy1[t] /. soln /. rts, yy2[t] /. soln /. rts}], {t, 0, 1, .01}],
  TableHeadings -> {None, {"x", "y"}}]


patte = TableForm[
  Table[Evaluate[{(r - yy6[t]) /. soln /. rts, -(yy7[t]) /. soln /. rts}], {t, 0, 1, .01}],
  TableHeadings -> {None, {"6", "7"}}]


patter = TableForm[Table[Evaluate[{yy1[t] /. soln /. rts}], {t, 0, 1, .1}],
  TableHeadings -> {None, {"x"}}]



lemon = Max[%]

w = 2 lemon


lily = (Part[endpt[P /. rts, d /. rts], 2] - d)
```

```
TableForm[
 Table[{t, Evaluate[yy1[t]], Evaluate[yy2[t]], Evaluate[yy3[t]], Evaluate[yy4[t]]},
  {t, 0, 1, .01}], TableHeadings -> {None, {"t", "xb", "yb", "θ", "Mb"}}]

numbers = TableForm[Table [
   {k, xb, P /. soln /. rts, d /. soln /. rts, Part[endpt[P /. rts, d /. rts], 2], lily},
   {u, u, u}], TableHeadings → {None, {"k", "xb", "P", "d", "h", "hu"}}]


Print[w]

chat = TableForm[Table[Evaluate[{yy7[y/(100 * r)] /. soln /. rts}], {y, 0, (r * 100), 1}],
  TableHeadings -> {None, {"y7"}}]



cha = TableForm[Table[Evaluate[{(yy6[1] - yy6[y/(100 * r)])} /. soln /. rts}],
   {y, 0, (r * 100), 1}], TableHeadings -> {None, {"y6"}}]
```

Loop Tack Test - With Contact Time Pulling Up

Shooting Method to determine variables p (horizontal force), mb (moment), θb(angle), sc(arc length), and q(vertical force).

Definition of variables:

q = vertical force applied at fixed end of elastica (one side only -referred to as r in the thesis body)

gP = initial guess for parameter P, horizontal force applied at fixed end of elastica

gMb = initial guess for parameter Mb, moment existing at peel front of bent elastica

r = contact length (one half of elastica) (referred to as b in the thesis body)

um = represents the maximum downward deflection

θb = angle at point B on the elastica

sc = arc length

k = relative stiffness

hi = height at inital contact

hp = height at end of pushing

hs = height during pulling (estimate)

Shooting Method

```
pi = N[Pi, 10]

r = 0.08

hi = 0.619378
hp = 0.448265
hs = 0.82

ht = hi + hs - 2 hp

maxη = 0.000664

um = (5 + 10 ht) * maxη

gP = 11.2

gθb = 0.30

gMb = 5.40

gq = -4.0

gsc = 0.82

k = 1000000

n = 3

B = 0.01
```

```
de[y3_, y4_, y5_, y7_, y8_, y9_, y10_, P_, q_] := {y1'[t] == y5[t] * Cos[y3[t]],
  y2'[t] == y5[t] * Sin[y3[t]], y3'[t] == y5[t] * (y4[t] + (B * (y4[t]^n))),
  y4'[t] == y5[t] * ((q * Cos[y3[t]]) - (P * Sin[y3[t]])), y5'[t] == 0,
  y6'[t] == (1 - y5[t]) * Cos[y8[t]], y7'[t] == (1 - y5[t]) * Sin[y8[t]],
  y8'[t] == -(1 - y5[t]) * (y9[t] + (B * (y9[t]^n))),
  y9'[t] == (1 - y5[t]) * ((P * Sin[y8[t]]) - (y10[t] * Cos[y8[t]])),
  y10'[t] == -(1 - y5[t]) * k * (y7[t] - um)}

leftBC[eb_, Mb_, sc_, q_] := {y1[0] == 0, y2[0] == 0, y3[0] == eb, y4[0] == Mb,
  y5[0] == sc, y6[0] == 0, y7[0] == 0, y8[0] == eb, y9[0] == Mb, y10[0] == q}

soln :=
 NDSolve[Flatten[Append[de[y3, y4, y5, y7, y8, y9, y10, P, q], leftBC[eb, Mb, sc, q]]],
  {y1, y2, y3, y4, y5, y6, y7, y8, y9, y10}, {t, 0, 1}, MaxSteps → 2200]

endpt[P_, Mb_, sc_, eb_, q_] :=
  {y1[t], y2[t], y3[t], y4[t], y5[t], y6[t], y7[t], y8[t], y9[t], y10[t]} /.
    First[NDSolve[Flatten[Append[de[y3, y4, y5, y7, y8, y9, y10, P, q],
        leftBC[eb, Mb, sc, q]]], {y1[t], y2[t], y3[t], y4[t], y5[t], y6[t],
      y7[t], y8[t], y9[t], y10[t]}, {t, 0, 1}, MaxSteps → 2200]] /. t -> 1;
endpt[
 gP,
 gMb,
 gsc,
 geb,
 gq]

Clear[P, Mb, sc, eb, q]

rts := FindRoot[{endpt[P, Mb, sc, eb, q][[3]] == pi / 2,
   endpt[P, Mb, sc, eb, q][[1]] == -r, endpt[P, Mb, sc, eb, q][[6]] == r,
   endpt[P, Mb, sc, eb, q][[8]] == 0, endpt[P, Mb, sc, eb, q][[10]] == 0},
  {P, {gP, 0.99 gP}}, {Mb, {gMb, 0.99 gMb}}, {sc, {gsc, 0.99 gsc}},
  {eb, {geb, 0.99 geb}}, {q, {gq, 0.99 gq}}, AccuracyGoal → 10, MaxIterations → 200]


rts

endpt[P /. rts, Mb /. rts, sc /. rts, eb /. rts, q /. rts]


P = P /. rts
            Mb = Mb /. rts
sc = sc /. rts
eb = eb /. rts
q = q /. rts

Print[P /. soln /. rts]
Print[Mb /. soln /. rts]

Print[sc /. soln /. rts]
```

```
Print[∂b /. soln /. rts]

Print[q /. soln /. rts]

{yy1[t_], yy2[t_], yy3[t_], yy4[t_],
  yy5[t_], yy6[t_], yy7[t_], yy8[t_], yy9[t_], yy10[t_]} =
 {y1[t], y2[t], y3[t], y4[t], y5[t], y6[t], y7[t], y8[t], y9[t], y10[t]} /. First[soln]

List[P /. rts, Mb /. rts, sc /. rts, ∂b /. rts, q /. rts,
 Part[endpt[P /. rts, Mb /. rts, sc /. rts, ∂b /. rts, q /. rts], 2],
 Part[endpt[P /. rts, Mb /. rts, sc /. rts, ∂b /. rts, q /. rts], 4]]

numbers = TableForm[
  Table [{k, P /. soln /. rts, Mb /. soln /. rts, sc /. soln /. rts, ∂b /. soln /. rts,
    q /. soln /. rts, Part[endpt[P /. rts, Mb /. rts, sc /. rts, ∂b /. rts, q /. rts], 2],
    Part[endpt[P /. rts, Mb /. rts, sc /. rts, ∂b /. rts, q /. rts], 4]}, {u, u, u}],
  TableHeadings → {None, {"k", "P", "Mb", "sc", "∂b", "q", "h", "Mc"}}]


bok2 = ParametricPlot[Evaluate[{yy1[t], yy2[t]} /. soln /. rts],
  {t, 0, 1}, PlotRange -> All, AspectRatio -> Automatic, PlotPoints -> 3000,
  GridLines -> Automatic, PlotStyle -> {{Thickness[0.02]}}]



bok3 = ParametricPlot[Evaluate[{(r - yy6[t]), -(yy7[t])} /. soln /. rts],
  {t, 0, 1}, PlotRange -> All, PlotPoints -> 3000,
  GridLines -> Automatic, PlotStyle -> {{Thickness[0.02]}}]



patterns = TableForm[
  Table[Evaluate[{yy1[t] /. soln /. rts, yy2[t] /. soln /. rts}], {t, 0, 1, .01}],
  TableHeadings -> {None, {"x", "y"}}]


patte = TableForm[
  Table[Evaluate[{(r - yy6[t]) /. soln /. rts, -(yy7[t]) /. soln /. rts}], {t, 0, 1, .01}],
  TableHeadings -> {None, {"6", "7"}}]


chat = TableForm[Table[Evaluate[{yy7[ y/(100 * r) ] /. soln /. rts}], {y, 0, (r * 100), 1}],
  TableHeadings -> {None, {"y7"}}]



cha = TableForm[Table[Evaluate[{(yy6[1] - yy6[ y/(100 * r) ]) /. soln /. rts}],
   {y, 0, (r * 100), 1}], TableHeadings -> {None, {"y6"}}]
```

APPENDIX C – LAB COMPARISON

Concurrently, with the analytical model that was developed, another student, Minh Le, conducted laboratory experiments of the loop tack test. In doing this research Ms. Le studied loops of different material backings. Her laboratory investigations began with using 1" x 12" strips of film of either mylar or polypropylene. The backings studied had different thicknesses of 2 mil, 5 mil, and 10 mil. The substrate used was a highly polished stainless steel panel of dimensions 2" x 6". Data and results can be seen in her report entitled, "Analysis of the Loop Tack Test Method for Pressure Sensitive Adhesives."

The second half of the research was conducted using metal feeler gauges of known thicknesses, since the material properties were known. These gauges had thicknesses of 4 mm, 5 mm, and 6 mm. The metal feeler gauges had no adhesive on them, but the adhesive was placed on the substrate and the feeler gauge was pressed down into the adhesive. This corresponds with the type of analysis conducted in the computer model as in chapters five and six.

The laboratory measured quantities display similar trends to those found for the data generated by the computer. The laboratory data for the feeler gauges shows a pushing down section, and a pulling up area. This corresponds to the type of data that was seen in the early chapters of this thesis. Shown below is a summary graph (Figure C.1) of the data found by Le. This graph corresponds very closely to the graphs shown in chapter six for $k= 10^6$ (Figure C.2). The graph is of force, measured in newtons, versus distance, measured in inches. The force corresponds to r in the computer analysis. The distance here refers to the distance the machine-head travels in pushing down to the substrate. This value corresponds to the h value, since the vertical distance traveled is related to the height of the top of the loop.

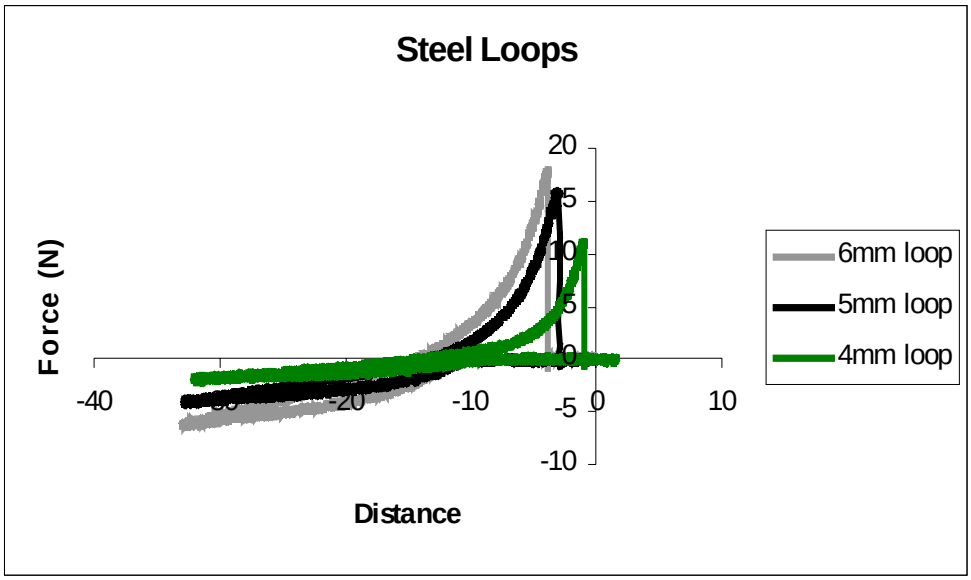

Figure C. 1. Force versus Distance – Laboratory Data

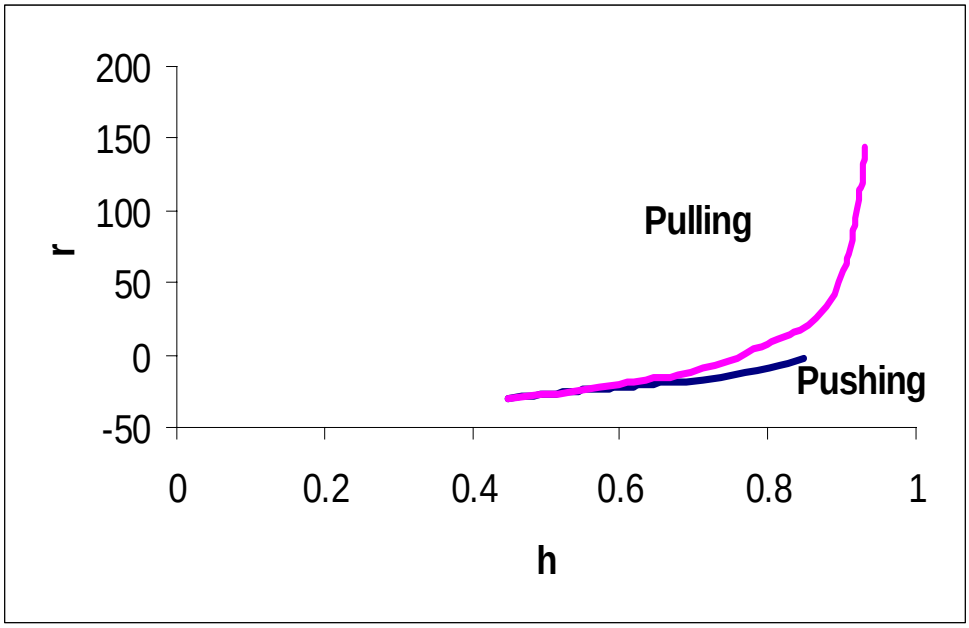

Figure C. 2. Force versus Height – Computer Data

Vita

NuRocha Lyn Williams, was born August 5, 1975 in Canandaigua, New York to Thaddeus and Martha Williams. She graduated from Irondequoit High School, in Rochester, New York, in June of 1993. In September of 1993 she began her university studies at Princeton University in Princeton, New Jersey. She graduated with her Bachelor of Science in Engineering degree in Civil Engineering in June 1997. After working for one year at Wegmans Food Markets, she went on to pursue a Master of Science degree in Civil Engineering at Virginia Tech, which was completed in June of 2000. She will begin work at Hayes, Seay, Mattern & Mattern, Inc. in Roanoke Virginia, as a structural engineer, focusing on building design.